EVALUATION OF STABILITY ANALYSIS METHODS OF EMBANKMENT ON SOFT CLAYS

Akzhunis Zhamanbay, MSc

School of Engineering

Department of Civil Engineering

Nazarbayev University

53 Kabanbay Batyr Avenue,

Astana, Kazakhstan, 010000

Supervisor: Jong-Ryeol Kim

Co-Supervisor: Sung-Woo Moon

December, 2018

Abstract

Construction on soft clay deposits is assumed to be a significant concern in the geotechnical engineering field. Soft clays are characterized by low bearing capacity, high ductility and low permeability, which lead to certain constraints in embankment design. Therefore, to ensure the safety of structures on soft grounds, it is necessary to define the capacity that the foundation can bear before the construction process. In addition, the behaviour of a structure has to be predicted to avoid failures or other unfavourable circumstances that could take place in the future. A number of prediction methods have been proposed, but the predictions could suffer from a lack of accuracy, resulting in a lack of confidence in practice. In this study, numerical simulation of embankments on soft soils using finite element method (FEM) is performed, along with the evaluation of existing methods for predicting the performance of embankments on soft clays and to propose the most accurate stability analysis approach among reviewed methods.

Keywords: soft clays, embankment, stability analysis, finite element method.

Acknowledgements

Firstly, I would like to express my profound gratitude and special thanks to my supervisor Prof. Jong Kim and co-supervisor Prof. Sung Moon, who helped me to develop this thesis work on the topic of "Evaluation of Stability Analysis Methods of Embankment on Soft Clays". Thanks to the guidance and assistance I received from them, the realisation of this project was possible.

I would like to acknowledge with appreciation the Nazarbayev University for giving me opportunity and perspective to conduct this thesis work.

I am extremely thankful to my parents and friends, who have supported and encouraged me at all times.

With best regards,

Akzhunis Zhamanbay

Table of Contents

List of Abbreviations and Symbols

B	Rratio of $\Delta u/\Delta \sigma'_v$ by Tavenas & Leroueil [18] method
c’	Cohesion of the soil
D	Depth of the soft soil layer
e_{cs}	Critical state void ratio of the soil
E_u	Undrained Young’s modulus of the soil
φ’	Friction angle of the soil
H	Embankment height
H_f	Embankment height at failure
κ	Swelling index of the soil
k_x, k_y	Permeability in x and y directions, respectively
λ	Compression index of the soil
LL	Liquid limit of the soil
M	Critical state parameter of the soil
ν	Poisson’s ratio
OCR	Overconsolidation ratio
p_i, p_f	Loads applied at the jth stage and at the failure, respectively, by Matsuo & Kawamura [6] method
PL	Plastic limit of the soil
s	Embankment settlement

s_{max}	Maximum settlement of the embankment
t	Embankment onstruction time
y	Lateral displacement
y_{max}	Maximum lateral displacement
γ	Unit weight of the soil
Δs_{max}	Incremental difference in maximum settlement under the embankment center
Δt	Incremental difference in time
Δu	Incremental difference in pore pressure
Δy_{max}	Incremental difference in maximum lateral movement measured embankment toe
$\Delta \sigma'_y$	Incremental difference in total applied vertical stress
P_c	Pre-consolidation pressure
θ	Angular distortion
WC	Water content of the soil

List of Tables

List of Figures

1 Introduction

1.1 Theoretical background

Construction on soft clay deposits is assumed to be an important concern in the geotechnical engineering field. Rapid development and increase in population make impossible avoidance of construction on soft ground. Certain characteristics of such soils, as low bearing capacity, lead to constraints in embankment load, properties as high ductility and low permeability, in turn, lead to high settlements, making the raised topic challenging [2]. Therefore, to design safe construction on soft grounds, it is necessary to define the capacity that the foundation can bear. In addition, the behaviour of the structure has to be predicted to avoid failures or other unfavourable circumstances. Safe design and prediction of foundation response for embankment construction also help to minimize the construction costs and duration [20]. Generally, accuracy in embankment design is achieved by applying different methodologies for evaluation of the stability, such as Limit Equilibrium Method (LEM) or Finite Element Method (FEM).

1.2 Aims & Objectives

The following work will be focused on the field of FEM based stability prediction methods. Along with stated methods, FEM software will be applied as well. Construction of appropriate model using software will lighten the struggles in the

prediction of embankment performance on soft clays, thus, helping to minimize both time and cost of construction.

Aims and objectives of the thesis work:

(i) Investigation of empirical evaluation methods of embankments on soft clays;

(ii) Collection of real-life data for analysis and numerical simulation;

(iii) Construction and simulation of the numerical model to observe the behaviour of the embankments on soft clays;

(iv) Validation of the numerical modelling by comparing the results with outcomes of the data;

(v) Determination of the most appropriate material model for numerical simulation;

(vi) Examination of the stability analysis methods by case studies;

(vii) Determination of the most appropriate method for prediction of the behaviour of the embankment constructed on soft clay;

(viii) Giving recommendations for further studies in the corresponding field.

The investigation will be conducted based on a stress-strain analysis. The model will be completed using staged construction method, to allow the strength gain of soil in every stage. The analysis will be done using a plane stress method since the length of the structure can be assumed as continuous. Thus, the 2D model will be appropriate for failure investigation.

1.3 Scope & Constraints

The simulation is conducted using various material models available in the Plaxis 2D software to investigate which describes soft clay the best. Evaluation is carried by validating the simulation output with the data obtained from case studies.

Since the research is based on numerical simulation, neither of laboratory equipment or materials are needed. Basic requirements include PLAXIS 2D software, library resources for literature review, and data sets for simulation. The software is available on university computers, as for library resources, enough information was found, despite the existence of several unavailable papers. From the literature review, 5 datasets were obtained for further analysis. Therefore, all resources are considered available, and the project does not have any expenses.

2 Literature Review

2.1 Embankment failure mechanisms

Typical embankment failure mechanisms are associated with the following aspects [1]:

(i) Bearing Capacity Failure. The collapse height of embankment is determined from a consideration of bearing capacity failure [19].

(ii) Rotational Failure. Rotational failure occurs when embankment height is less than or equal to the height of embankment. Failure occurs along

a circular arc that goes through the underlying soil and the embankment fill.

(iii) Sliding Failure. In the sliding failure, slope portion slides laterally as a rigid body due to active pressure acting on it.

(iv) Spreading Failure. In this failure, soil wedge slides due to the active pressure acting [19].

(v) Foundation Soil Squeezing Failure. In soft soils consisting of several layers, a layer that has a low strength can be the location of the horizontal sliding plane. This mechanism may be favoured where stiff crest overlies soft soil or where the thickness of soft soil is small. The failure takes place at the point when the distributed load is higher than the resisting force.

(vi) Failure Due to Interaction Effect. The performance of structure not founded on soft soil like bridges and extension of the old embankment is affected by the behaviour of adjacent structures on soft soil due to negative skin friction

2.2 Factors affecting stability of embankments on soft ground

According to RDSO [1], stability analysis of embankments on soft clays aims to guarantee the safety of the embankment and prevent the collapse, caused by the shear failure. Stability investigation is conducted using observational approaches that collect data from earth structures with installed instrumentation. Application

of settlement plates, survey monuments, extensometers, inclinometers and piezometers help to monitor the settlement and stability of embankments. Figure 2.1 below illustrates the idealized embankment section with installed monitoring tools.

Stability of embankments and ground conditions are affected by various factors. Indicators of certain points have to be collected that are shown in Figure 2.1. Analysis, in most cases, is carried taking into account the following aspects [7]:

(i) Height. Embankment height gives an opportunity to measure the load exerted.

(ii) Vertical deformation at the toe (Point 2) and at the point beyond toe (Point 3) of the structure.

(iii) Pore water pressure. Excess pore water pressure under the centre and toe of the embankment. Due to the partial consolidation of the clay foundation during construction, the vertical effective stress generally reaches the pre-consolidation pressure during construction. As a consequence, the excess pore pressures to dissipate after construction are given by the difference between the final effective stress profile and the pre-consolidation pressure profile [13].

(iv) Settlement under embankment centre (Point 1).

(v) Lateral deformation. Lateral displacement at embankment toe (Point 2) is assumed to be related to the occurrence of embankment failure. The

lateral displacement has a direct relationship with the effective stress pattern during and after construction. They can relatively simply be related to settlements [13].

(vi) Angular distortion. Deformation at the toe of the structure measured using inclinometers.

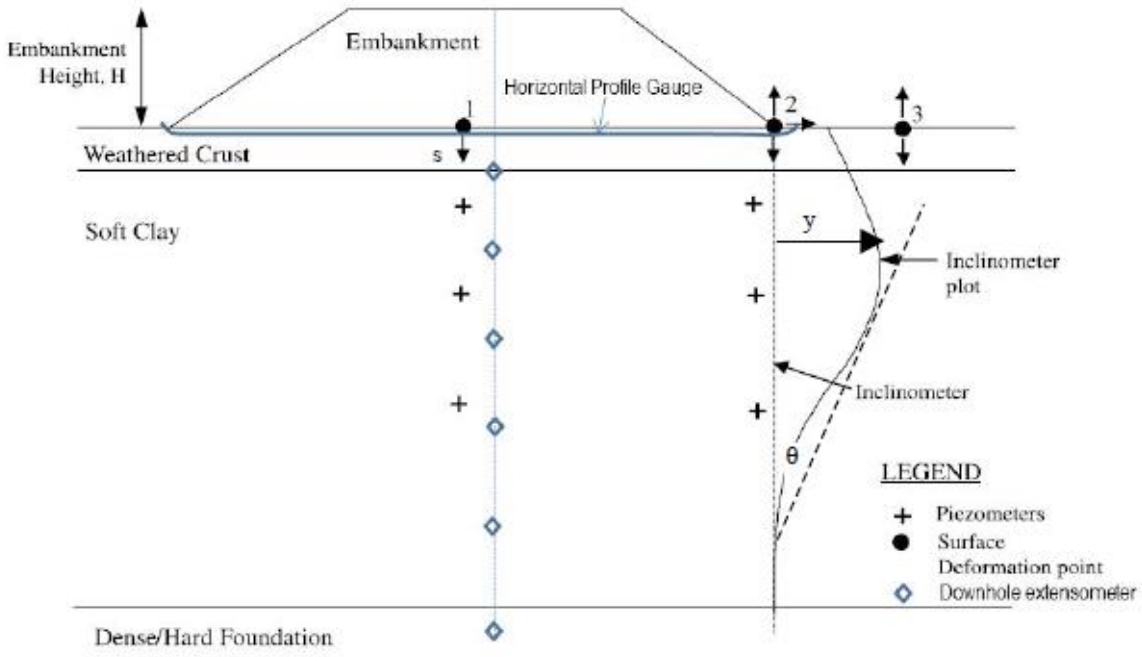

Figure 2.1 Idealized section of embankment indicating the types of monitored observations [7]

2.3 Stability analysis methodologies

Numerous stability analysis methods were developed in the last decades. The predictions were made using data from observations. Researchers have suggested different methods referring to a number of factors and several of them will be analyzed using numerical modelling.

Observational methods have always been used by engineers working in the fields now included in applied soil mechanics, but ‘the observational method’ is a term having a specific restricted meaning. In its complete and ultimate form, the observational method provides a distinct and possibly novel approach to design. [15]. The observational approach consists of monitoring of pore pressures and deformations, usually with reference to the calculated factor of safety. For most slopes, e.g. constructed cuts, fills, dams and embankments on soft clay, monitoring is used as a back-up to the factor of safety design, i.e. as a check on the assumptions, rather than as a primary design tool [16].

LEM has been used extensively to assess the short-term (undrained) stability of reinforced embankments constructed on soft foundation soils. These methods have been used mainly to examine the equilibrium of a slip circle type failure mechanism passing through the embankment fill and foundation soil [14].

The limit equilibrium and plasticity solutions provide no information about deformations or strains, which develop in the basal reinforced embankment system. To investigate the interaction behaviour between the foundation soil, the reinforcement, and the embankment fill a well as the strains and deformations of the system, numerical methods, typically finite element methods, are used [14].

2.4 Review of existing empirical methods

The method proposed by Matsuo and Kawamura [6] is to plot maximum embankment settlement (s_{max}) versus the ratio of incremental changes of

maximum lateral displacement to settlement ($\Delta y_{max}/\Delta s_{max}$) (Figure 2.2). P_j and P_f in the legend table of the figure correspond to loads at the j^{th} stage and at failure, respectively. Contour lines are presented for different ratios of these loads. The higher the load ratio, the more severe the crack or the more unstable the embankment. Authors suggest taking as a standard P_j/P_f = 0.9 since surface cracking was observed at this value. They also mention that the method might not be applicable to all sites.

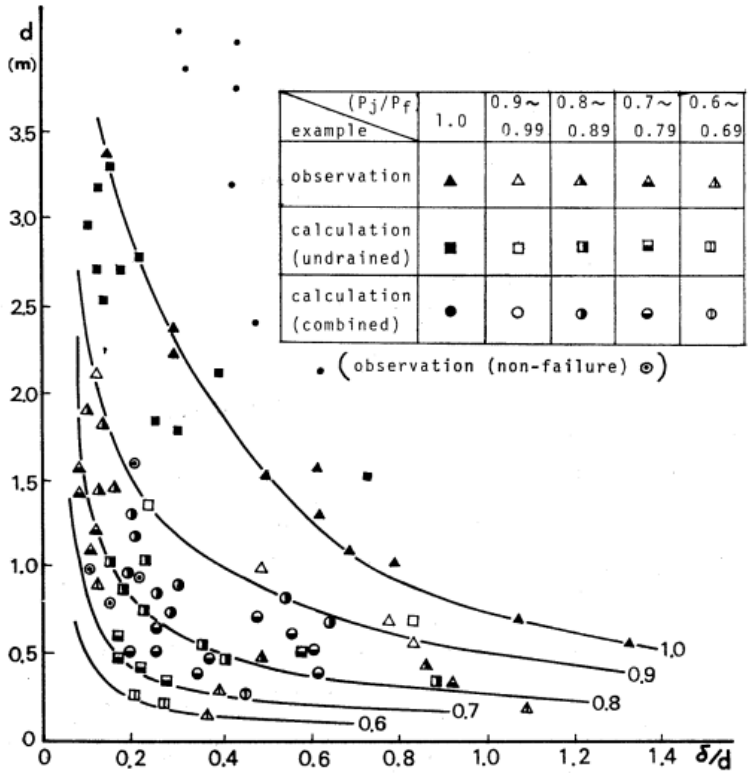

Figure 2.2 Embankment failure contour lines [6]

According to Todo et al [17], Kurihara and Ichimoto proposed to evaluate the failure of the embankment on soft ground based on the rates of lateral displacement at embankment toe. Even though there are many other factors affecting this relationship, such as soil condition, embankment shape and

construction methodology, certain lateral displacement rates (20 to 30 mm/day) are considered to cause minor cracks on the embankment. Todo et al [17] also mention the embankment construction control method suggested by Tominaga and Hashimoto, which is also based on lateral displacement. This method uses a plot of embankment settlement against lateral displacement (Figure 2.2). It can be observed that the slope of the graph undergoes rapid changes before a crack occurrence.

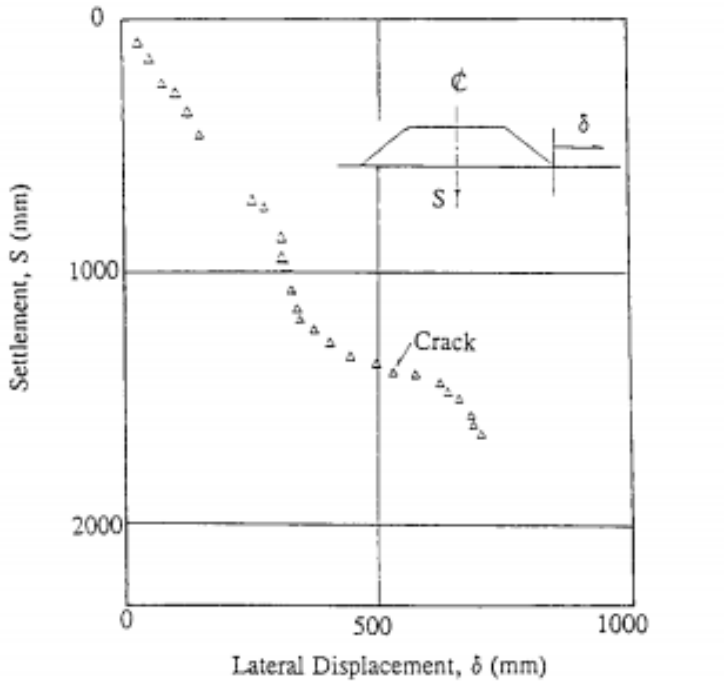

Figure 2.3 Application example of diagram for construction control of embankment [17]

The use of lateral deformation monitoring to predict impending embankment failure is relatively more commonly studied. Calvacante, Coutinho and Gusmao [3] provided a summary of available methods for this purpose and illustrated the use of horizontal displacement methods via several case studies in Brazil.

Coutinho and Bello [4], consequently, summarized their previous studies using lateral displacements to analyze the embankment stability and identified several failure criteria. Methodologies are based on investigations of

(i) maximum lateral displacement,

(ii) maximum lateral displacement normalized by the layer thickness (failure > 1.2 %), and

(iii) rate of maximum lateral displacement normalized by the layer thickness versus time (failure > 0.2 %/day). Authors recommended using several methods to assure the analysis results.

Calvacante, Coutinho and Gusmao [3] also propose to use the angular distortion at the embankment toe and plot the similar graph as in the application of lateral displacement. In other words, the divergent plot of the

(i) maximum angular distortion against time (failure > 3%),

(ii) the rate of the maximum angular distortion against time (failure > 1.5 %/day).

Ortigao, Werneck and Lacerda [8] recommend plotting the maximum lateral displacement normalized by the maximum embankment height against the embankment height normalized by the maximum embankment height. They observe the slope of the graph and assume that 2.7 % ratio indicates the approaching failure.

The method proposed by Tavenas and Leroueil [18] is one of the widely known approaches for embankment stability evaluation. It also uses the slop of maximum settlement vs maximum lateral displacement plot to define the stability boundaries. The study concluded that the following conditions could be used as limits to avoid embankment failure,

(i) $y_{max}/s_{max} = 0.18 \pm 0.09$ – within pre-consolidation pressure of soil;

(ii) $y_{max}/s_{max} = 0.91 \pm 0.20$ – above pre-consolidation pressure of the soil (undrained condition)

(iii) $y_{max}/s_{max} = 0.16 \pm 0.02$ – at the end of construction (consolidation of the soil)

Authors also predict the slope failure using effective vertical stress and excess pore water pressure. The embankment is assumed to be not stable when the slope of the plot is higher than 1 (Figure 2.4) [18].

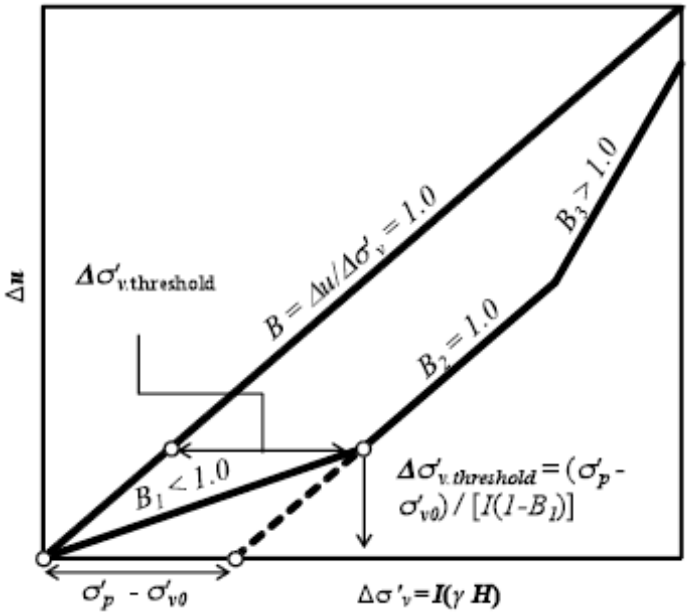

Figure 2.4 Excess pore pressure vs effective vertical stress [18]

Another method, by Hunter and Fell [7], is analyzing a range of factors and concluding with the following indicators:

- A rate of lateral displacement at the toe of the embankment is considerably increased with an approach of the failure condition when height is between 70-90% of failure height
- Heave, or vertical deformation at toe and point beyond toe, is observed at 60-90% of failure height and can describe the impending failure condition
- Maximum angular distortion is increasing at 70-90% of failure height.

Since all three criteria are based on relative height, only the first approach will be used with an assumption of 70% of failure height as a failure point.

Trani and Wong [5] are plotting the rate of inverse incremental horizontal deformation at the toe of embankment versus the height of embankment. The prediction is based on extrapolation of data, to determine the failure height (inverse rate ratio is 0). The point where inverse incremental horizontal deformation rate reaches approximately 0.05 days/mm or above is referred to as a failure.

The next proposed method is derived from the following reasoning:

(a) It is known that two clay layers having the same profile $C_u(z)$ but different geological origins may have different behaviours when identically loaded and

may fail for different heights of embankments having the same geometry. Therefore, Bjerrum's correction factor is applied to enhance accuracy.

(b) The author states that two clay layers having the same profile σ'y will fail in the same way when they are loaded (undrained condition) in the same way, even if they have different C_u [10].

Table 2.1 represents the summary of the reviewed methods.

Table 2.1 Summary of existing methods of stability analysis

#	Failure indicators	Authors
1	Plot of maximum embankment settlement (s_{max}) versus the ratio of incremental changes of maximum lateral displacement to settlement ($\Delta y_{max}/\Delta s_{max}$)	Matsuo and Kawamura [6]
2	Plot of rates of lateral displacement at embankment toe	Kurihara and Ichimoto [17]
3	Plot of embankment settlement against lateral displacement at the toe of embankment	Tominaga and Hashimoto [17]
4	Plot of the maximum angular distortion vs time Plot of the rate of maximum angular distortion vs time	Calvacante, Coutinho and Gusmao [3]
5	Plot of maximum lateral displacement normalized by maximum embankment height vs embankment height normalized by maximum embankment height	Ortigao, Werneck and Lacerda [8]
6	Plot of maximum embankment settlement against maximum lateral displacement at the toe of embankment. Plot of effective vertical stress versus excess pore water pressure	Tavenas and Leroueil [18]
7	Rate of lateral displacement at the toe of embankment is considerably increased with approach of failure condition, when height is between 70-90% of failure height	Hunter and Fell [7]

	Heave, or vertical deformation at toe and point beyond toe, is observed at 60-90% of failure height, and can describe the impending failure condition	
	Maximum angular distortion is increasing at 70-90% of failure height.	
8	Plot of maximum lateral displacement normalized by the layer thickness vs time	Coutinho and Bello [4]
	Plot of the rate of maximum lateral displacement normalized by the layer thickness vs time	
9	Plot of the rate of inverse incremental horizontal deformation at the toe of embankment versus the height of embankment	Trani and Wong [5]
10	Ultimate loading of the embankment can be calculated by equation, $P_{ult} = \gamma H_f = N_{\emptyset o'} \sigma_{p'}$	Otoko [10]

2.5 Plaxis 2D

The following study will be conducted by means of numerical simulation on Plaxis 2D software. PLAXIS 2D with additional modules 2D Thermal, 2D Dynamics and 2D PlaxFlow is a powerful and convenient finite-element software package designed for two-dimensional deformation and stability analysis of geotechnical structures. It has a user-friendly graphical interface that encourages fast learning of the user. The software helps to construct the model of soils, foundations and etc., to simulate the constructed model under applied conditions, and to analyze the model using automatically generated finite element mesh [2].

Since the cases that will be covered during this study concern the embankments construction, Plaxis 2D is comparably suitable for the application, as the length of the embankment could be considered as continuous. The analysis is can be conducted using the results of last stage, calculation. The software is able to

choose a specific point to evaluate before calculation stage, and the result for chosen points are obtained after calculation. The model is constructed using staged construction method [21].

The results of the simulation could be derived for total and principal stresses, deformation, and etc. The results are illustrated in the form of counter maps or vectors, from which soil behaviour and movement could be observed [21]. Stress-strain and deformation related simulation results of the earth structures are the essential information for the prediction of structure stability/failure conditions [1]. Thus, Plaxis 2D gives a wide range of opportunities for analysis of geotechnical structures with required data.

PLAXIS is used throughout the world by leading design companies and institutes in the field of civil and industrial construction for modelling excavations, embankments, foundations, tunnels, deposits and storage [2].

2.6 Model development

2.6.1 Material models

Model for investigation will be constructed for 5 data sets and different material models, as it was mentioned before. Plaxis 2D software database offers an opportunity to choose the suitable material models that are characterized by mechanical deformation behaviour of the soil. Among proposed models, Mohr-Coulomb, Hardening Soil, Soft Soil, and Modified Cam Clay material models will

be considered for simulation of variant soil behaviours for given thesis work taking into account characteristics of the soft clay.

(i) Mohr-Coulomb model (MC). It is a linear-elastic perfectly plastic material model. It requires 5 input parameters of soil for simulation, such as Young's modulus (E) and Poisson's ratio (ν) for soil elasticity, soil friction angle (φ) and cohesion (c) for soil plasticity, and angle of dilatancy (ψ). It is assumed to be the first-order approximation of soil or rock behaviour and recommended for application in the first analysis of the chosen case. The stiffness of the layers are, generally, considered to be constant or increasing with depth linearly. Therefore, the computations with the MC model are comparably fast and convenient for the first calculations.

(ii) Hardening Soil model (HS). It is assumed to be a more advanced way for simulation of ground conditions. Similar to MC model, the stresses of the model could be given by soil friction angle (φ), cohesion (c), and angle of dilatancy (ψ), whereas the stiffness of the structure is described in more details with three inputs for higher accuracy: triaxial loading stiffness (E50), triaxial unloading stiffness (Eur ≈ 3E50), and the oedometer loading stiffness (Eoed ≈ E50). The stiffness parameters described are dependent on pressure. In addition, attention should be paid to initial soil conditions, as they are important in soil deformation problems.

(iii) Soft Soil model (SS). It is a special model for clayey soils of near normally-consolidated state. It is, mainly, used for primary compression analysis. The

model is comparably similar with HS model, except the fact that SS is more accurate for simulation of soft soils.

(iv) Modified Cam-Clay model (MCC). It is a widely used model for modelling of soft soils. MCC model is used for simulation of near normally-consolidated clayey soils and for comparison with other codes.

The software also offers an opportunity to choose the soil conditions based on its ability to drain and bear the applied load to increase the accuracy of the simulation.

2.6.2 Staged construction method

When the shear strength of the soil is low, it is impossible to construct embankments with large surcharge or height. In such cases the construction is, generally, carried out in several stages, thus, allowing strength gain in time between subsequent stages. It is called the staged construction method and widely used in construction on soft grounds [12].

Generally, embankments can be constructed safely in one stage only in the case of very flat slope or wide sub-banks, which ensure the stability of the structure. These options are assumed to not effective in terms of cost management since the amount of material used is considerably larger. Therefore, the staged construction approach is practised to have both stable and economic structure. The main reasoning of the staged construction method is the fact that it allows the soft soil to gain strength by increasing the load gradually without failure. The gain in shear

strength is a function of the angle of shearing resistance improved in terms of effective stress parameters and degree of consolidation [1].

Similarly, the model for given thesis work will be developed using staged construction method. It is carried out in the last part of model development in “staged construction” tab, where the construction stages are differentiated using multiple phases.

3 Case studies

3.1 Muar test embankment, Malaysia [23]

The test site was developed by the Malaysian Highway Authority with the purpose of detailed investigation of the Muar clay. As a result, multiple test embankments were constructed, among which one was developed to observe embankment failure. An overall average thickness of the Muar clay constitutes 20 m with a max depth of 25 m. The test embankments are constructed 20 km inland Malaysian in the direction of the southeast coast. The soil profile revealed that there exists a 2.0 m thick weathered crust layer above the soft clay layer with the thickness of 16.5 m. The soft silty clay layer consists of 2 layers: lower soft silty clay layer overlaid by an upper very soft clay layer. The dense sand layer is observed at the depth of 22.5 m below the ground level. The peaty soil layer with the thickness of 0.3-0.5 m is located immediately above the sand layer. Generally, the majority of the soft clays observed in Malaysia tends to normally consolidated, however, the

investigation revealed that the weathered crust layer is overconsolidated. It could be reasoned by soil weathering and dessiciation. The overconsolidation ratio of the layers can reach very high numbers, thus, resulting in high preconsolidation pressure and low shear stress. (Figure 3.1).

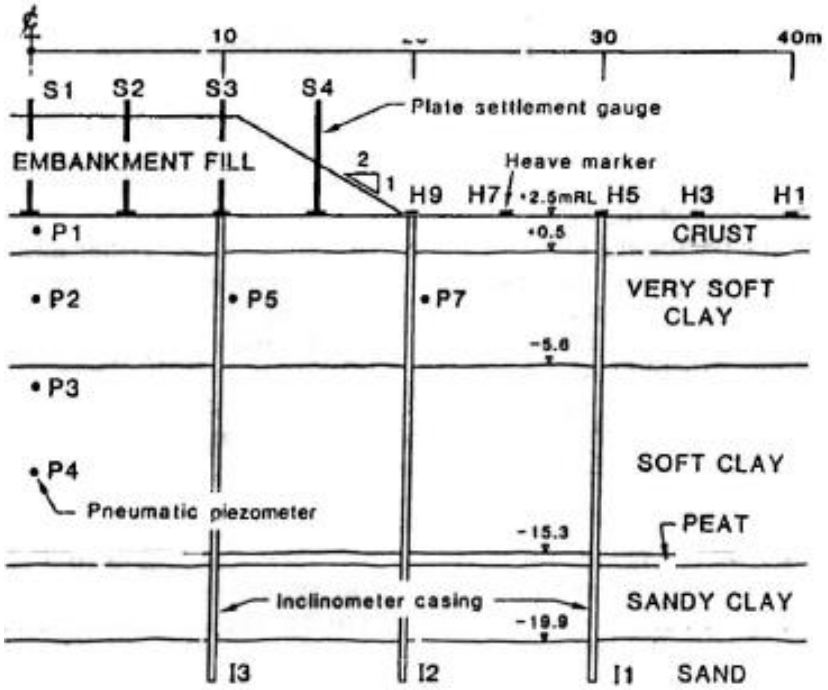

Figure 3.1 Cross section of the Muar test embankment [23]

As it was mentioned earlier, one of the test embankments at the Muar site was constructed to failure. It was found that the embankment failed at the height of about 5.5 m with rotational (quasi slip circle) failure. The crack was observed to be vertically propagating through the embankment crust and fill. The site parameters are shown in Table 3.1.

Table 3.1 Soil parameters at the Muar test site [23]

#	Layers	Depth, m	WC, %	LL, %	PL, %	γ, kN/m^3	ϕ', °	e_{cs}	ν	λ	κ	c', kPa	Eu, kPa	Pc, kPa	OCR	kx, m/d	ky, m/d	M
1	Weathered crust	-0.5	83	110	40	16.5	12.5	3.1	0.3	0.2	0.05	8.0	25500	110	5.64	1.30E-04	6.91E-05	1.19
2	Very soft silty clay with decated leaves and roots	-5.5	100	90	35	16.5	12.8	3.1	0.3	0.4	0.05	12.5	13685	40	0.77	1.30E-04	6.91E-05	1.19
3	Soft silty clay with traces of shell fragments occasionally sand lenses	-15.3	73	85	40	15.5	16.3	2	0.3	0.3	0.08	15.0	6619	60	0.57	1.05E-04	5.68E-05	1.10
4	Peaty soil	-15.9	-	-	-	-	-	-	-	-	-	-	-	-	-	-	-	-
5	Sandy silt/clay with organic matters	-19.9	50	70	30	16	21.5	1	0.3	0.2	0.09	14.0	5884	60	0.45	9.50E-05	5.18E-05	1.05

3.2 Yongsan river embankment, Korea [24]

The thickness of the soft ground is 15m up to 25m in average, and the thickness of the soft layer is getting deeper in the direction of Namchangcheon and Yongsan River. The thickness of the soft layer on the right side is slightly deeper than that on the left side.

The sedimentary clay soil distributed in the soft ground of the Yongsan River estuary is in unified classification and the calcination state is in the intermediate calcination state.

The state of the embankment in the study area is summarized as follows Table 3.2. The first embankment was started on December 11, 2006, at a height of 0.79 m, and the crack occurred the height was 6.4 m on April 16, 2007. After such event 1.6 m was removed to maintain 4.8 m On January 29th, the final embankment was carried out at 7.14m.

Table 3.2 Construction stages of the Yongsan river embankment [24]

Stage	Date	Increments, m	Height, m	Rest period, day	Comments
1	11.12.2006	0.79	0.79	63	
2	12.02.2007	1.05	1.84	30	
3	14.03.2007	1.71	3.55	26	
4	09.04.2007	2.47	6.02	7	sliding
5	16.04.2007	0.38	6.4	8	crack
6	24.04.2007	-1.6	4.8	48	
7	11.06.2007	1.35	6.15	232	
8	29.01.2008	0.99	7.14	322	
end	16.12.2008				

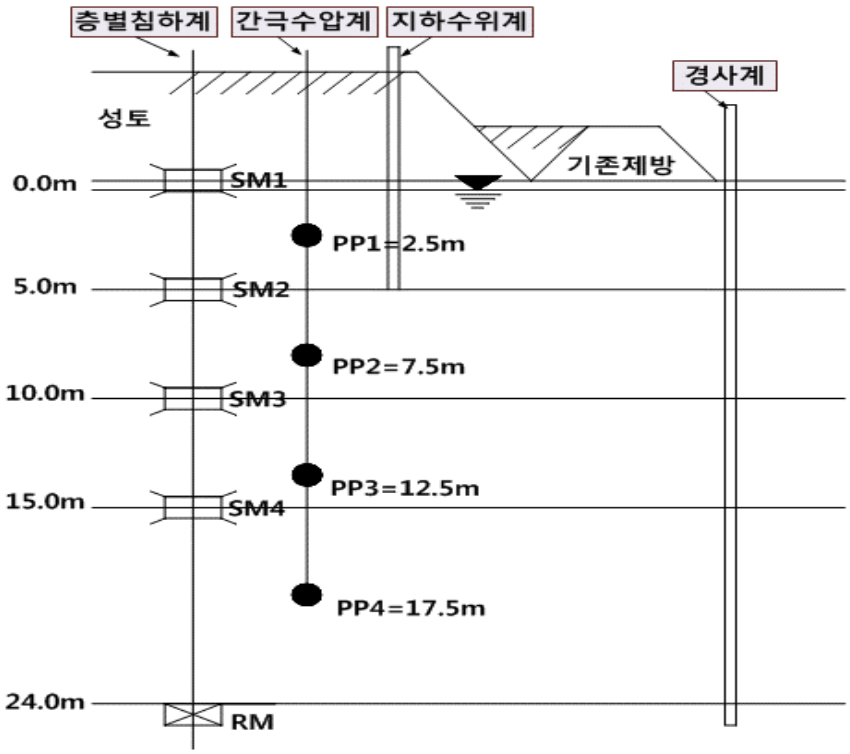

Figure 3.2 Cross section of the Yongsan river embankment [24]

3.3 West Java fill, Indonesia [17]

West Java fill is a preload fill in Indonesia presented by Todo et al [17]. The site consists of 12 m soft clay over stiff clay layer. There is a 4 m crust over the soft clay, as well. Compared to other case studies, West Java site has lower water contents, with liquid limits around 100% and plastic limits around 35 %.

All layers have comparably high strength according to field vane strength investigation, which varies between 25-50 kPa for soft layers and more than 80 kPa at the stiff clay layer. Therefore, the fill height reached 12 m until the failure occurred. The construction started June 30, 1992, and finished after 3 months,

September 22, 1992. The settlement and lateral displacement at the failure were 1188 mm and 473 mm, respectively.

3.4 Sarapui test embankment, Brazil [22]

The Sarapui testing site is situated in a very flat swampy area, locally known as "Fluminense Plains," which covers a surface area of about 150 km2 around Guanabara Bay, Brazil. At the site, the clay deposit is about 11 m thick and overlies sand and gravel layers (Figure 3.3). The clay layer consists of the kaolinitic group clays with size content of 65 %.

An indication that the embankment approached failure was observed firstly when the height reached 2.5 m. It was a 1 cm wide crack along the embankment crest. However, the instrumentation did not show any sign of the crack at this moment. At the next construction stage, when the height was lifted to 2.8 m, severe crack was observed on both the embankment crest and the instrumentation readings.

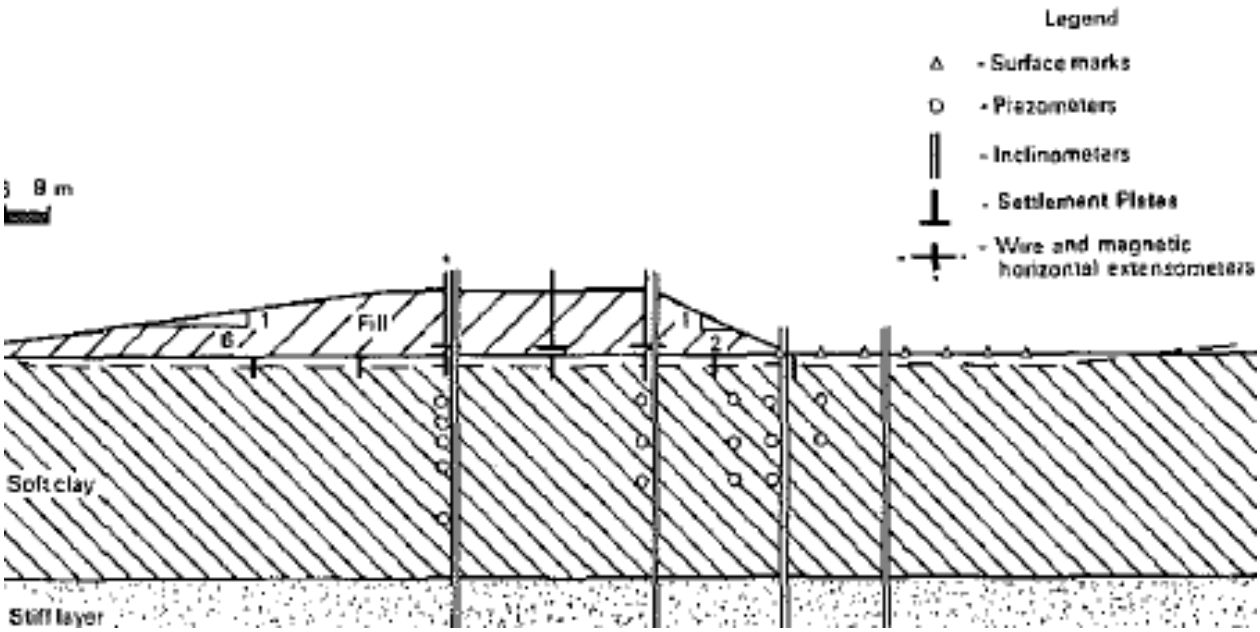

Figure 3.3 Cross section of the Sarapui test embankment [22]

3.5 Juturnaiba test embankment, Brazil [4]

The Juturnaíba Dam Project, an embankment structure located in the Northern portion of the State of Rio de Janeiro, in Brazil, was built from 1981 to 1983. The Project included the Juturnaíba trial embankment and the Juturnaíba Dam construction. The two cases are located in areas with similar geotechnical characteristics. The foundation consisted basically of an organic clay deposit about 8 m thick, with SPT values (blows/length in cm) ranging from 0/111 to 1/33, typically 0/50, along its full depth, underlain by sand sediments with SPT values about 10/30, reaching a depth of 14 m. Visual classification and laboratory tests permitted division of the clayey deposit into six layers, with variations in organic and water content, ranging from light-grey silt clay to brown clayey peat (Figure 3.4).

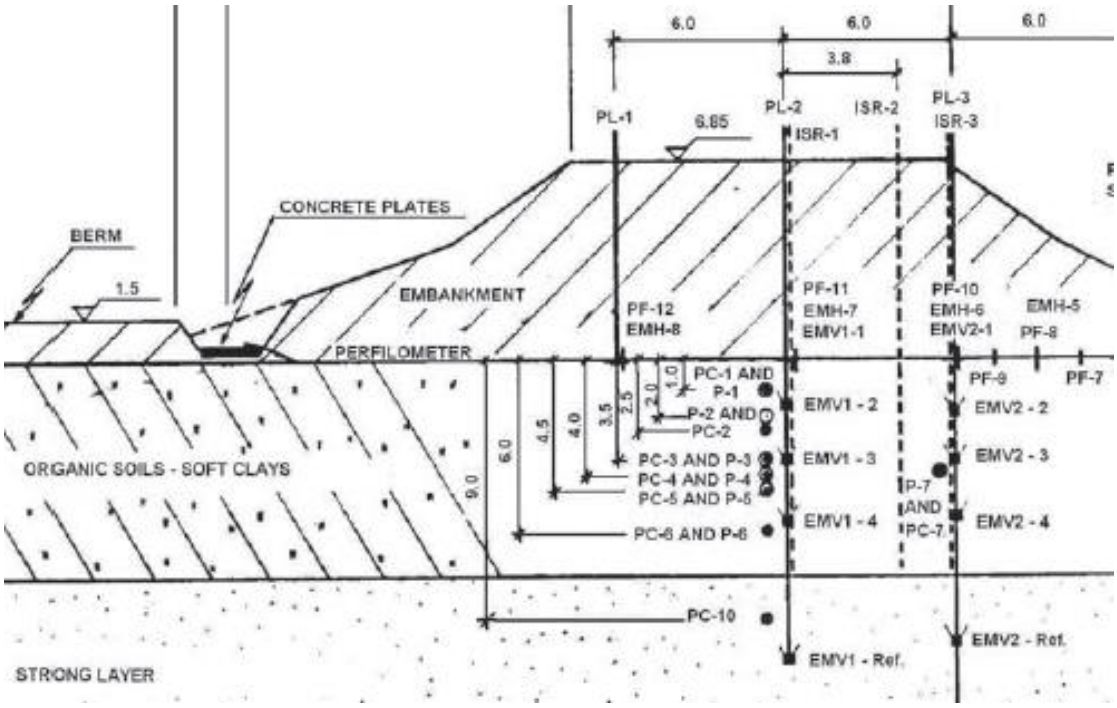

Figure 3.4 Cross section of the Juturnaiba test embankment [4]

The figure 3.5 below, summarizes the information about the test embankments that are required for the further analysis.

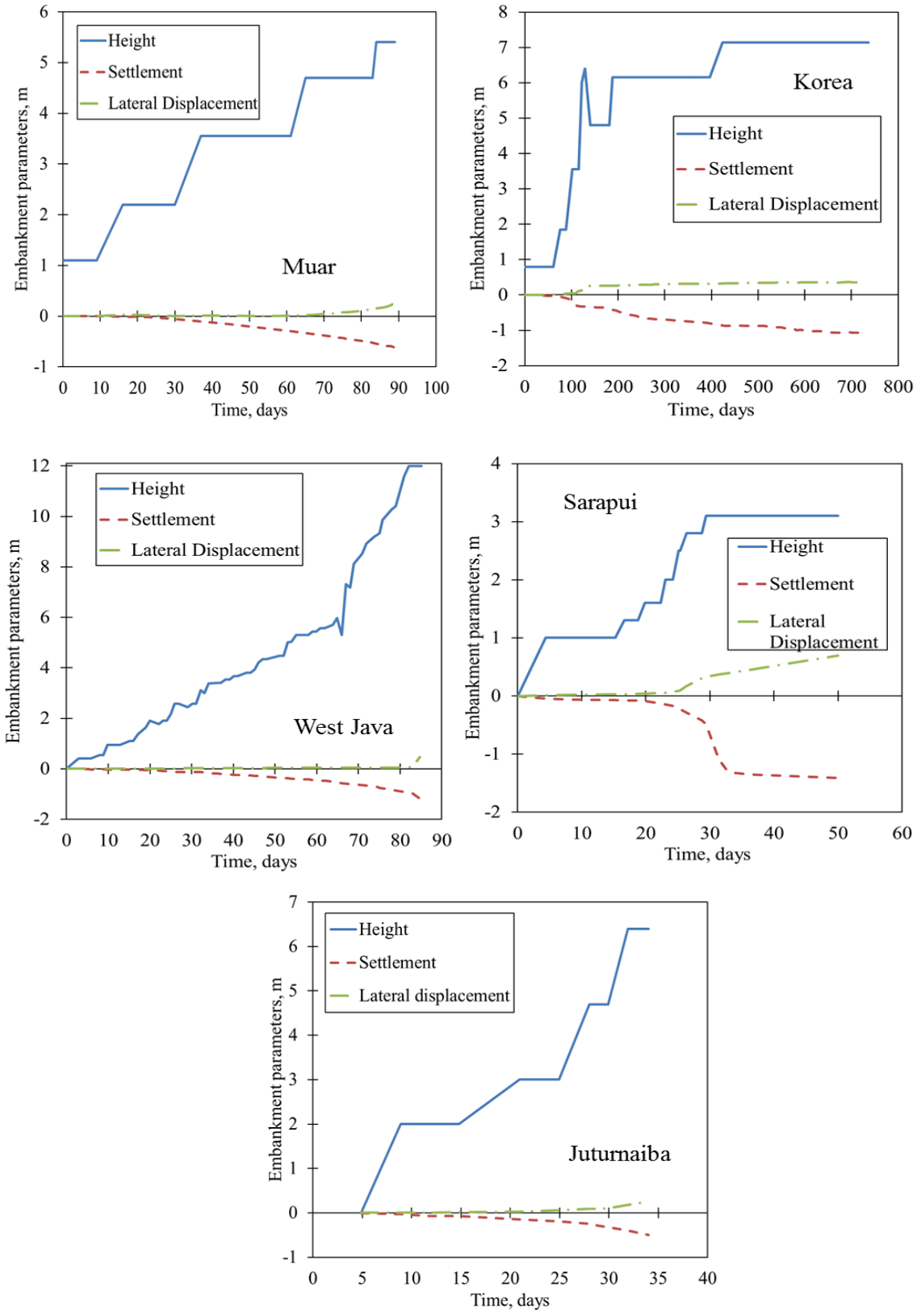

Figure 3.5 Embankment parameter for all case studies.

4 Numerical simulation

Numerical simulation carried out for Muar test embankment is presented.

4.1 Adaptation of raw data for soft material models

The soil parameters required as input for Plaxis 2D is given by Table 3.1. The Table 4.1 below shows the parameters required to adapt to different material models. The initial void ratio was derived from the critical state void ratio using equation (1) [25],

$$e_0 = \frac{\gamma - \gamma_{dry}}{\gamma_w - \gamma + \gamma_{dry}}, \quad (1)$$

where γ is the bulk unit weight;

γ_{dry} is the dry unit weight;

γ_w is the unit weight of water.

The pre-overburden pressure (POP) is found using equation (2) [25],

$$POP = P_c - \sigma', \quad (2)$$

where P_c is the pre-consolidation pressure;

σ' is the vertical effective stress (= (γ - γ_w) * h).

Mohr-Coulomb and Modified Cam Clay constitutive models do not need any additional input parameters. Plastic straining due to primary deviatoric loading (E^{ref}_{50}), plastic straining due to primary compression (E^{ref}_{oed}), and elastic unloading/reloading (E^{ref}_{ur}) required for Hardening Soil model are found in

accordance to literature review. Modified compression (λ*) and swelling (κ*) indexes are needed for both Hardening Soil and Soft Soil models are found by equation (3) and (4), respectively,

$$\lambda^* = \frac{\lambda}{1+e_0}, \quad (3)$$

$$\kappa^* = \frac{\kappa}{1+e_0}, \quad (4)$$

where λ and κ are compression and swelling indexes.

Table 4.1 Additional parameters for adaptation

#	Layers	e_0	λ*	κ*	E^{ref}_{50}, kPa	E^{ref}_{oed}, kPa	E^{ref}_{ur}, kPa	POP, kPa
1	Weathered crust	2.9	0.061	0.013	5247	1639.7	15741	90.5
2	Very soft silty clay with decated leaves and roots	4.7	0.084	0.009	7619	1190.5	22857	12
3	Soft silty clay with traces of shell fragments occasionally sand lenses	1.9	0.108	0.035	1913	925.5	5738	45.9
4	Peaty soil	-	-	-	-	-	-	-
5	Sandy silt/clay with organic matters	0.8	0.111	0.106	632	900	1895	73.5

The embankment was constructed following the case study (Appendix A). The base width is 45 m with two levels:

(i) 2.5 m high, 15 m wide berm;

(ii) 3 m high, 14 m wide berm.

The slope of both levels is 1:2.

As it was mentioned in literature review, the construction was carried out in several stages, each consisting of lifting and resting (Table 4.2). In total 11 stages of construction constituted 20 phases in Plaxis 2D simulation. The total construction duration is 90 days and the final embankment height is 5.5 m.

Table 4.2 Construction stages of Muar test embankment

Stage	Date	Increments, m	Height, m	Rest period, day	Duration, days	Phase
1	09.11.1988	0.6	0.6	4	4	0
	Rest stage		0.6	4	8	
2	13.11.1988	0.5	1.1	4	12	1
	Rest stage		1.1	14	26	2
3	19.11.1988	0.5	1.6	6	32	3
	Rest stage		1.6	4	36	4
4	22.11.1988	0.6	2.2	3	39	5
	Rest stage		2.2	7	46	6
5	29.11.1988	1.35	3.55	7	53	7
	Rest stage		3.55	16	69	8
6	01.12.1988	0.45	4	2	71	9
	Rest stage		4	4	75	10
7	04.12.1988	0.35	4.35	3	78	11
	Rest stage		4.35	4	82	12
8	05.12.1988	0.35	4.7	1	83	13
	Rest stage		4.7	1	84	14
9	06.12.1988	0.25	4.95	1	85	15
	Rest stage		4.95	1	86	16
10	07.12.1988	0.35	5.3	1	87	17
	Rest stage		5.3	1	88	18
11	08.12.1988	0.2	5.5	1	89	19
	Rest stage		5.5	1	90	20

In order to eliminate errors due to width of the foundation, the most optimal values were selected using the method of trials. Table 4.3 shows the output for foundation width selection. As a result, 150 m was chosen, since the settlement and lateral displacement indicators have insignificant changes for subsequent options.

Table 4.3 Foundation width selection

L (m)	s_{max} (mm)	y_{max} (mm)
100	464.4	233.6
150	464.6	234.4
200	464.6	234.5
250	464.6	233.9

Similar approach was used to identify the most optimal mesh size, as well. The finest available option for mesh size “very fine” has mesh dimensions of 0.5. Therefore, to achieve more accurate results, expert settings were applied, and mesh size was decreased to 0.35 (Figure 4.1). Finer mesh size led to increase of simulation duration at not significant changes in results.

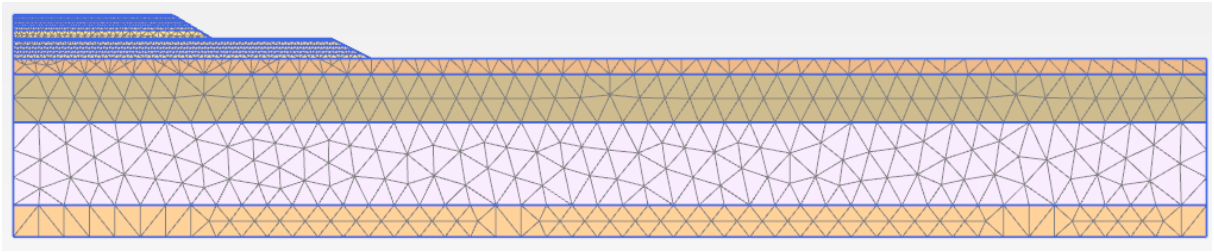

Figure 4.1 Plaxis 2D mesh

4.2 Validation of the simulation

The simulation was carried out for 4 different constitutive soil models under the same construction stages. In all simulations, failure occurred at the last stage as in

the field case. However, in MC, MCC, and SS models' simulations failure is occurring during the resting part of the last stage (phase 20), whereas in HS model simulation failure take place at lifting part (phase 19), a little earlier.

The results in terms of settlements under the embankment centre and lateral displacements at the embankment toe are illustrated in Figures 4.2 and 4.3 along with the data from the field. It can be observed that the settlement profile is quite similar, unlike the lateral displacement profile. It is assumed to be the result of possible errors due to construction stages since in the field every stage is levelled using a bulldozer. From Figure 4.2 it can be seen that all material models, except for MC are showing a little lower values that the field data. The lowest settlement is observed in the MCC model. Both the closest profile and the value is resulting from the SS model.

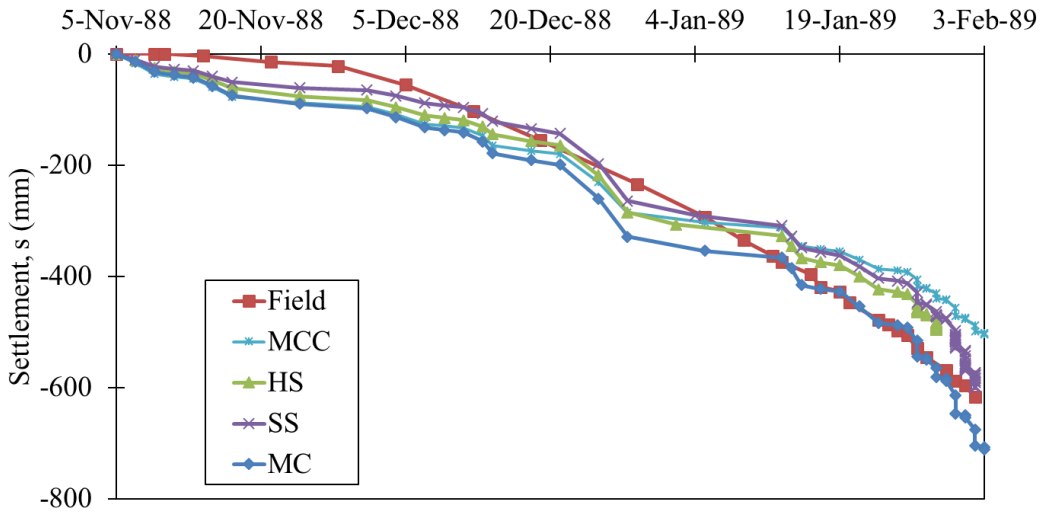

Figure 4.2 Comparison of settlements for all material models

In case of lateral displacements, all models except for SS are showing much lower values, the lowest being HS model. In terms of graph profile, the largest difference is observed in MCC model. Similarly, the best results among analyzed in terms of graph profile and maximum values are given by SS model.

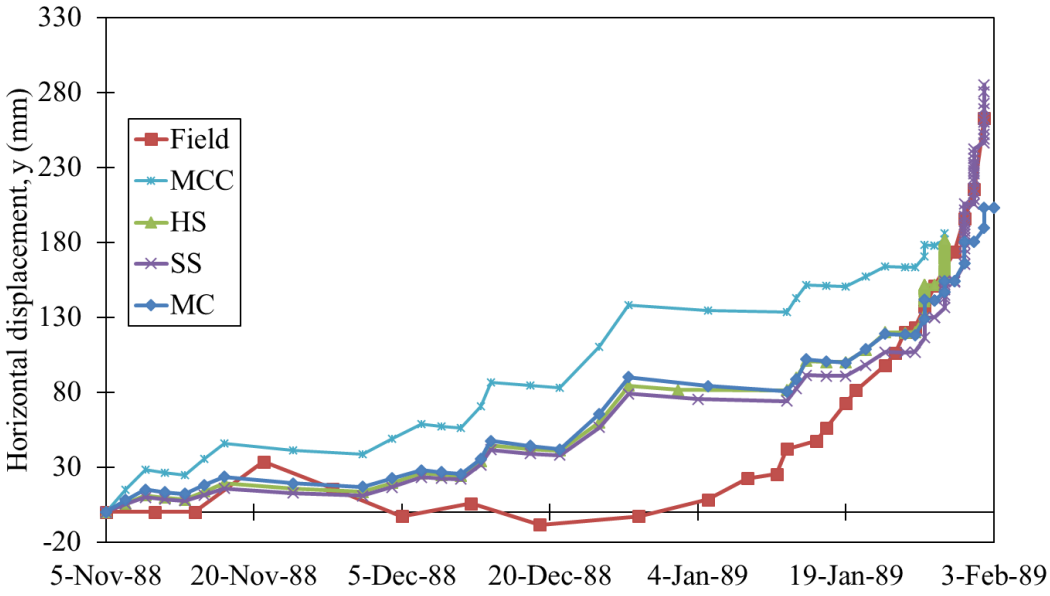

Figure 4.3 Comparison of lateral displacements for all material models

Table 4.4 presents the numerical comparison of the soil constituve models with the field data. Since the differences are not significant, the least suitable model to describe the settlement profile of embankment constructed on soft clays cannot be chosen. Nevertheless, it can be assumed that the HS model is the least suitable to characterize the behaviour of the soft clay in terms of the lateral displacement at embankment toe. The lowest differences in both settlements and lateral displacements are observed in SS model. Thus, most accurate material model to characterize the soft clay using Plaxis 2D software is assumed to be the soft soil model.

Table 4.4 Comparison of results for all material models

	s (mm)			y (mm)		
Field	-616.3	|Δ|	(%)	262.9	|Δ|	(%)
MC	-482.7	133.6	21.7%	300.1	37.1	14.1%
MCC	-504.0	112.3	18.2%	211.6	51.3	19.5%
HS	-495.9	120.4	19.5%	181.3	81.6	31.0%
SS	-600.5	15.8	2.6%	285.1	22.1	8.4%

More detailed simulation outputs for each soil constitutive model are given in the Appendix A.

5 Application of empirical stability prediction methods

5.1 Matsuo and Kawamura [6]

Figure 5.1 illustrates the application of Matsuo and Kawamura counter lines to all 5 data sets. As it was stated before, the higher the load ratio, the more unstable the embankment. The point where the plot intersects with counter lines are points that show the characteristics of the failure. However, it does not necessarily the failure point. The point where any crack event is observed is referred to as failure. In cases of Muar and Juturnaiba test embankments, a small crack is occurring as the plot gradually approaches 0.8 counter line at the last stage (final point).

In West Java fill, at the penultimate point there is no crack, since it is lower than 0.7 counter line. Consequently, at the last point, there is a very rapid change that leads to severe crack (higher than 0.9). Sarapui test embankment shows the

occurrence of the small crack when the plot reaches 0.8, followed by severe crack when it reaches 0.9 counter line.

In Korean field case, a small crack is observed when the plot is higher than 0.7. The slope of the graph is divergent due to unloading and reloading.

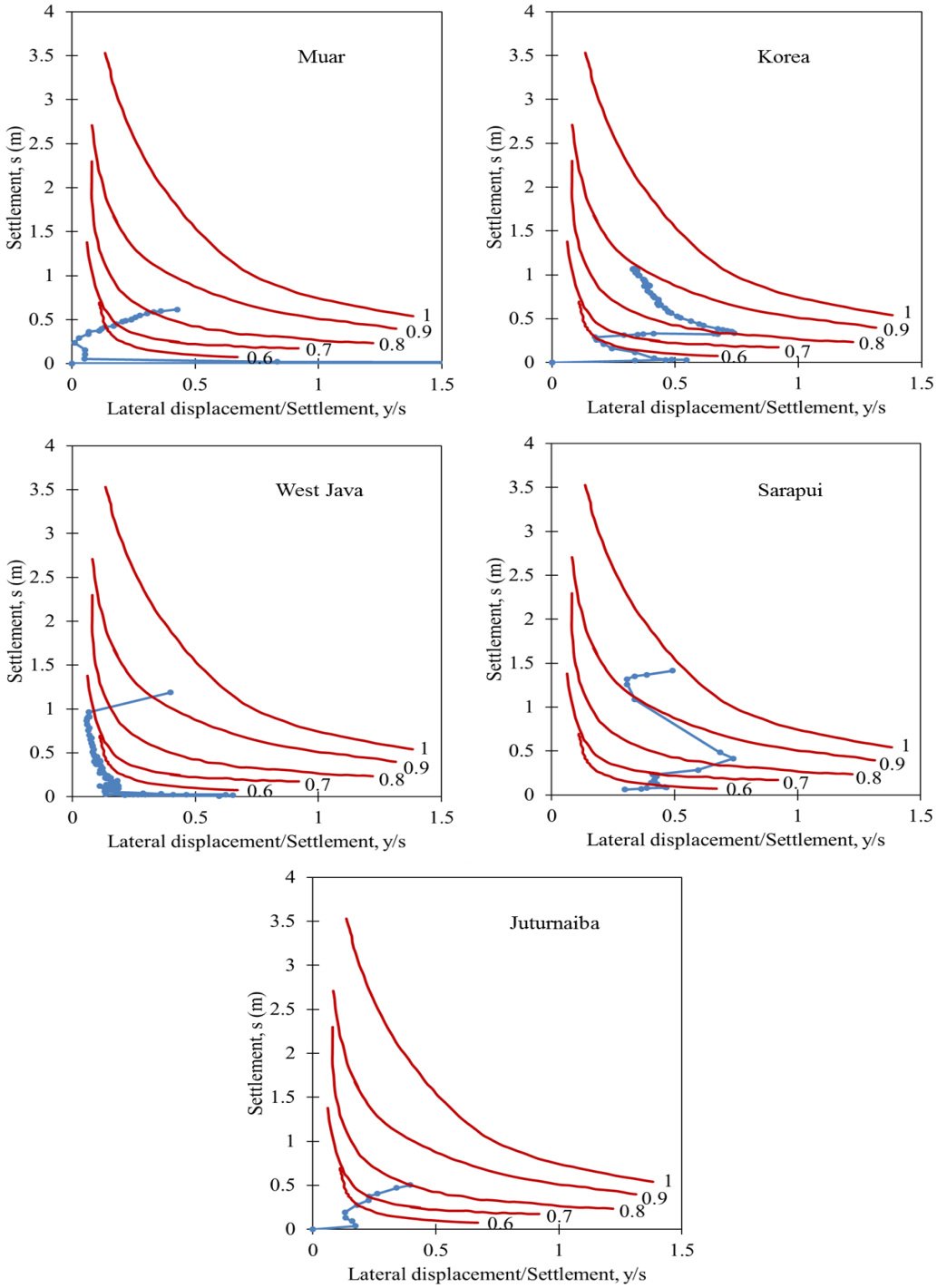

Figure 5.1 Failure analysis of all 5 datasets using Matsuo and Kawamura counterlines

5.2 Kurihara and Ichimoto [17]

The point where the rate of the lateral displacement reaches 20 mm/day (min is taken) is assumed to be failure point. Therefore, in the Figure 5.2 below, on the plots of lateral displacements versus time the slope ratios at the failure and just before the failure are illustrated. From the Figure 5.2, the sudden crack of the West Java fill can also be observed, as the slope rapidly increases from 4.3 to 232 mm/day. The Korean case can also be referred to as comparably rapid crack, as its rate changes from 1.6 to 23.9 mm/day. It can be seen that in other 3 cases the rate of the lateral displacement changes gradually, as it approaches the failure.

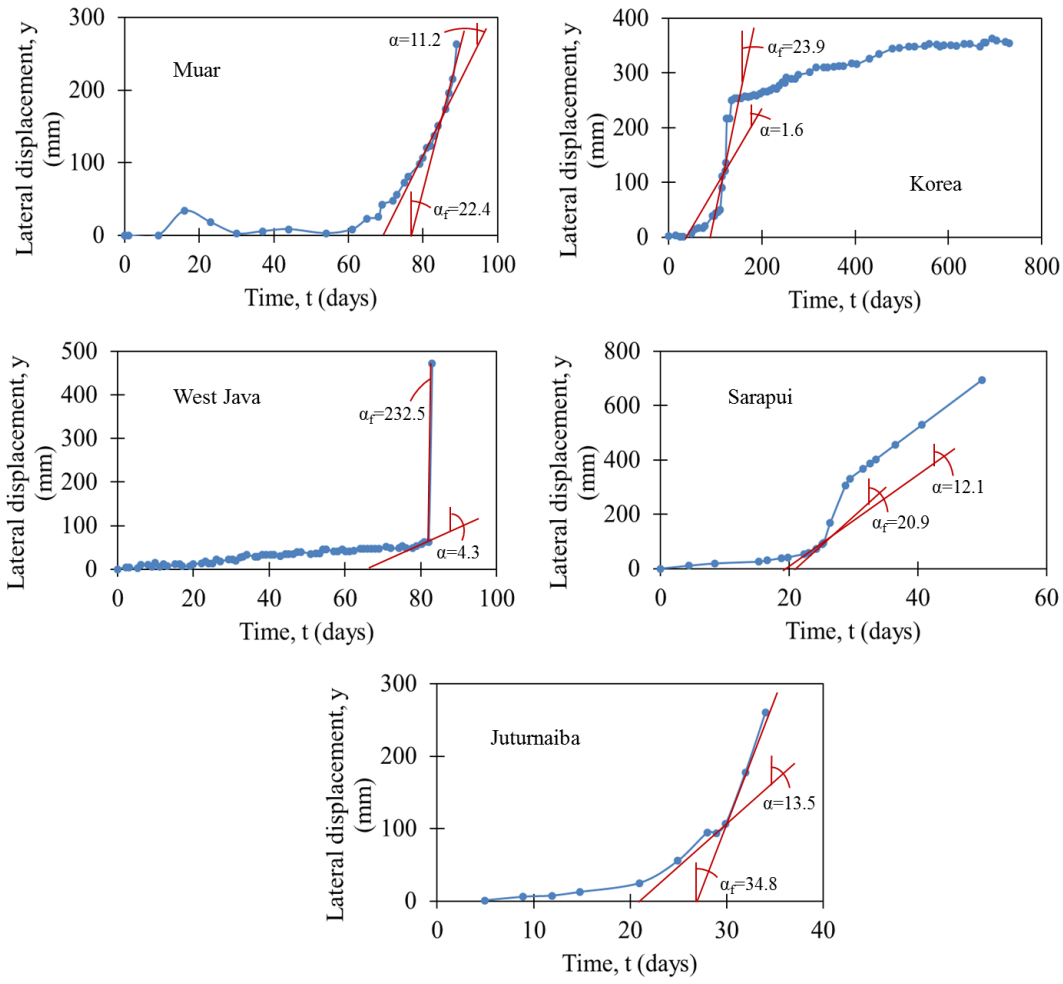

Figure 5.2 Failure analysis plot of all 5 datasets by Kurihara and Ichimoto

5.3 Tominaga and Hashimoto [17]

According to the failure criteria by Tominaga and Hashimoto, the slope of the plot should be higher than 0.7 or higher than initial slope + 0.5. Therefore, the initial slopes, the slope at failure and at the point before the failure are shown. Following the directions:

(i) Muar: $\alpha_f = \alpha_0 + 0.5 > 0.7 \Rightarrow \alpha_f = 0.78+0.5=2.28 > 0.7$

Thus, $\alpha_f > 2.28$.

The failure occurs at the penultimate stage with $\alpha_f = 2.33$.

(ii) Korea: $\alpha_f = \alpha_0 + 0.5 > 0.7 \Rightarrow \alpha_f = 0.19+0.5=0.69 < 0.7$

Thus, $\alpha_f > 0.7$.

The failure occurs with the rapid change from $\alpha = 0.52$ to $\alpha_f = 2.69$. The observed value is much higher than the failure criteria.

(iii) West Java: $\alpha_f = \alpha_0 + 0.5 > 0.7 \Rightarrow \alpha_f = 0.58+0.5=1.08 > 0.7$

Thus, $\alpha_f > 1.08$.

The failure occurs with the rapid change from $\alpha = 0.26$ to $\alpha_f = 1.82$. The observed value is much higher than the failure criteria.

(iv) Sarapui: $\alpha_f = \alpha_0 + 0.5 > 0.7 \Rightarrow \alpha_f = 0.39+0.5=0.89 > 0.7$

Thus, $\alpha_f > 0.89$

The failure occurs with the gradual change from $\alpha = 0.46$ to $\alpha_f = 1.43$.

(v) Juturnaiba: $\alpha_f = \alpha_0 + 0.5 > 0.7 \Rightarrow \alpha_f = 0.04+0.5=0.54 > 0.7$

Thus, $\alpha_f > 0.7$.

The failure occurs at the penultimate stage with $\alpha_f = 0.97$.

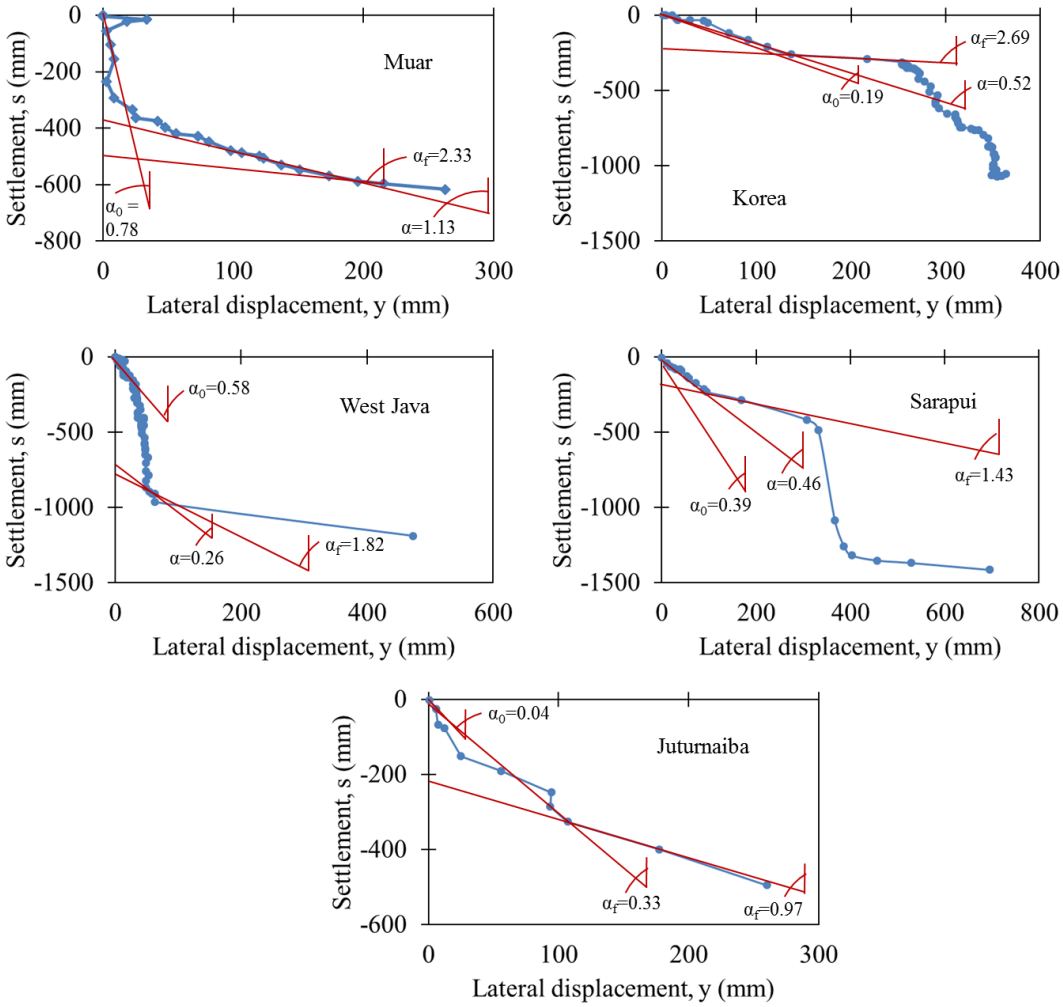

Figure 5.3 Failure analysis of all 5 datasets by Tominaga and Hashimoto

5.4 Calvacante, Coutinho and Gusmao [3]

Given methodology uses the angular distortion at the embankment toe. The angular distortion is derived from the lateral displacement. Therefore, similar trends can be observed. Figure 5.3 shows the divergent plot of the angular distortion vs time, where the point where the value of the θ is higher than 3 % is referred to as failure. The failure is detected in cases of Sarapui, West Java and

Juturnaiba test embankments. The methodology could not detect failure in cases of Muar and Korean embankments.

Application of the failure criterion based on the rate of the angular distortion ($\Delta\theta_f/\Delta t$ = 1.5 %/day) is also shown at the failure point from the first criterion. It revealed that according to the second criterion the failure is occurring earlier in Sarapui and Juturnaiba test embankments in comparison to the first. The failure at the Muar and Korean embankments could not be detected, as well.

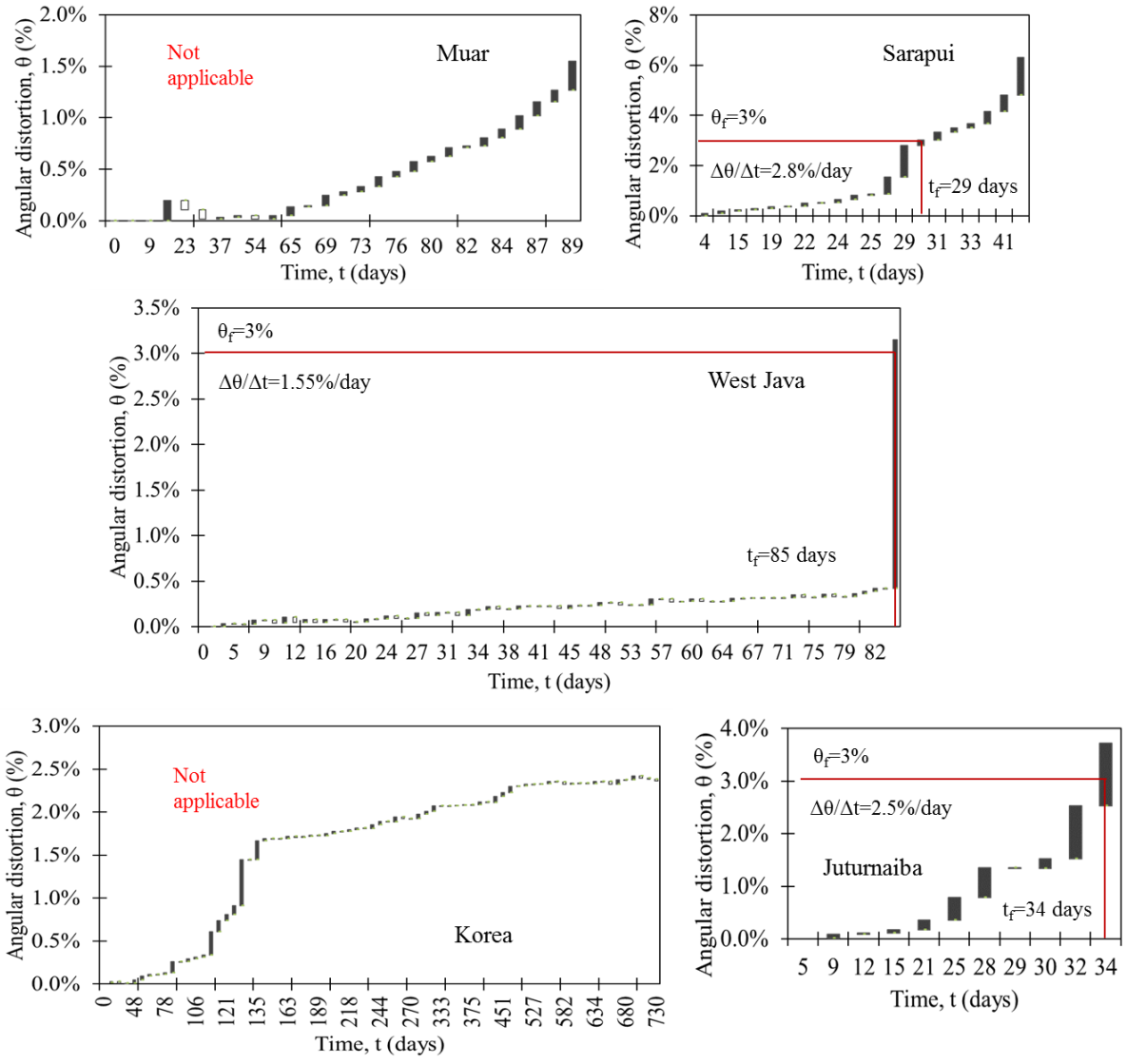

Figure 5.4 Failure analysis of all 5 datasets by Calvacante, Coutinho and Gusmao

5.5 Ortigao, Werneck and Lacerda [8]

The failure criterion is based on the slope of the plot, which is α > 2.7 %. The slopes of the plot at the point before failure and at the failure point are shown in Figure 5.5. It can be seen that in all cases, except for West Java site, the plots are gradually approaching the failure, since no sudden changes are observed. In Sarapui case, only the failure slope is illustrated, because the changes were too insignificant. The graph of the Korean case is not convergent due to unloading/reloading.

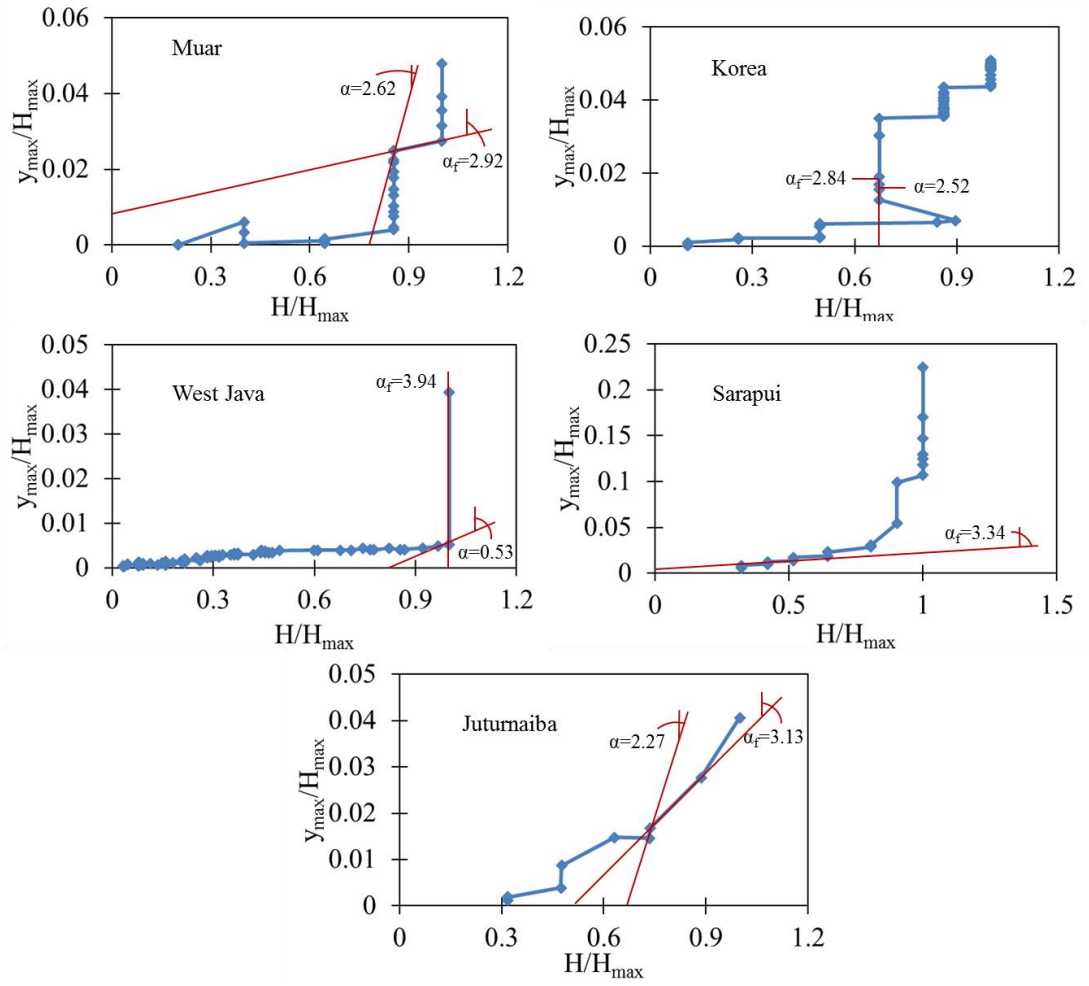

Figure 5.5 Failure analysis of all 5 datasets by Ortigao, Werneck and Lacerda

5.6 Tavenas and Leroueil [18]

The methodology proposed by Tavenas and Leroueil [18] consists of two different failure criteria, of which the first is similar to Tominaga and Hashimoto method. Both methodologies use the plot of the settlement against lateral displacement and failure criteria based on the slope of the plot. The difference being the critical value of the slope (α_f = 0.91 for undrained condition). Therefore, only the second failure criterion based on the excess pore pressure is presented (Figure 5.6). The point where the slope of the excess pore pressure vs effective vertical stress plot becomes more than 1 is referred to as failure (the red line in the figures indicate the limiting slope of the plot).

The methodology could not detect failure in case of Muar and Korean embankments. In these cases, the points where the failure should have occurred are shown. It can be seen that the values of B are not too small, but less than 1. Which could indicate the issues with accuracy of the failure criterion.

In West Java and Sarapui embankments, the failure is occurring suddenly, with the change from B=0.2 to B=1.3 or B=1.2, respectively.

In Juturnaiba test embankment, failure is the slope of the plot is increasing gradually. It reaches the failure when the slope increases from B=0.8 to B=1.2.

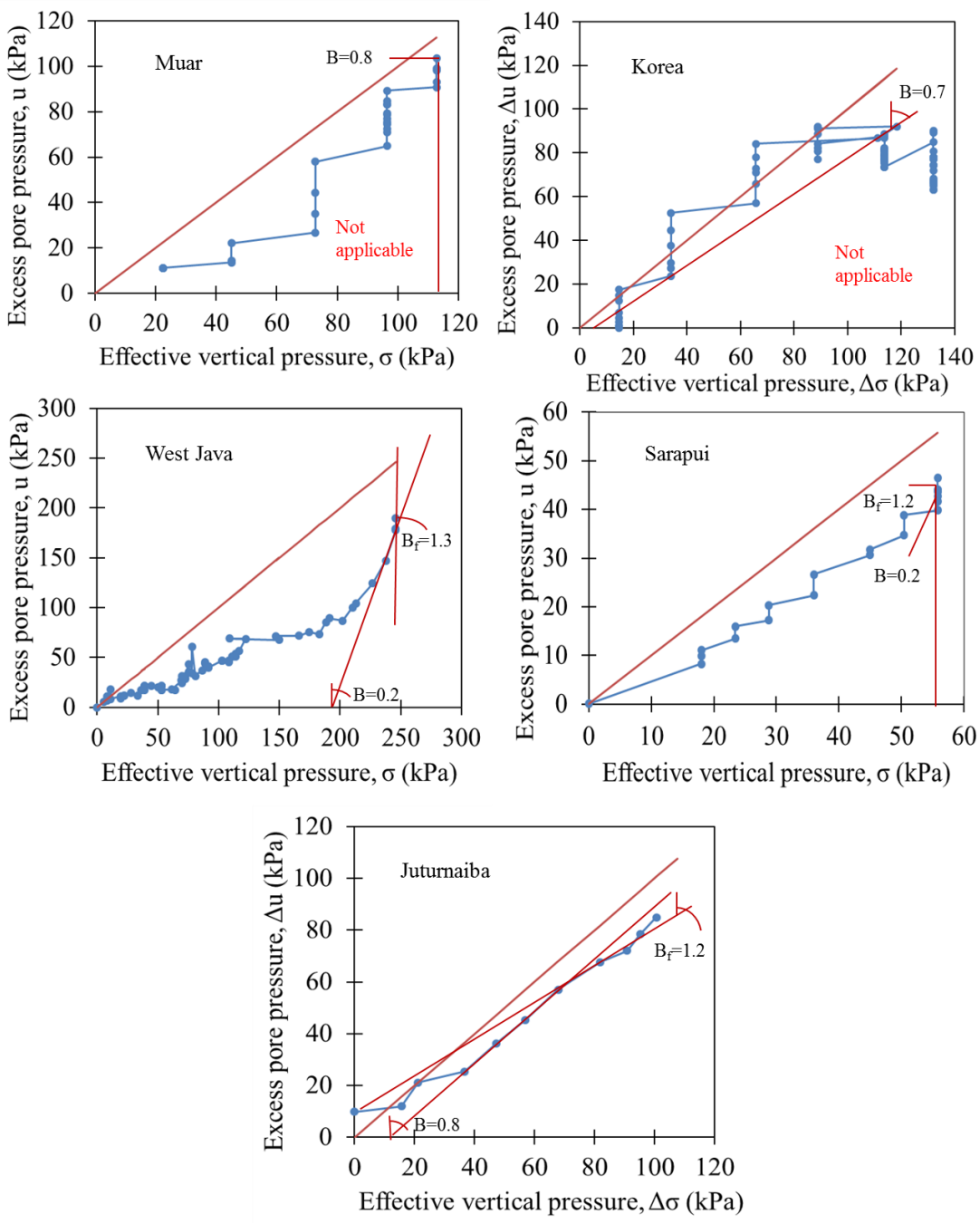

Figure 5.6 Failure analysis of all 5 datasets by Tavenas and Leroueil

5.7 Hunter and Fell [7]

The methodology proposed by Hunter and Fell is based on the observation that in most cases, embankment approaches the failure when its height reaches 70% of

the failure height. Therefore the points when the relative height is 0.7 are indicated as failure points (Figure 5.7).

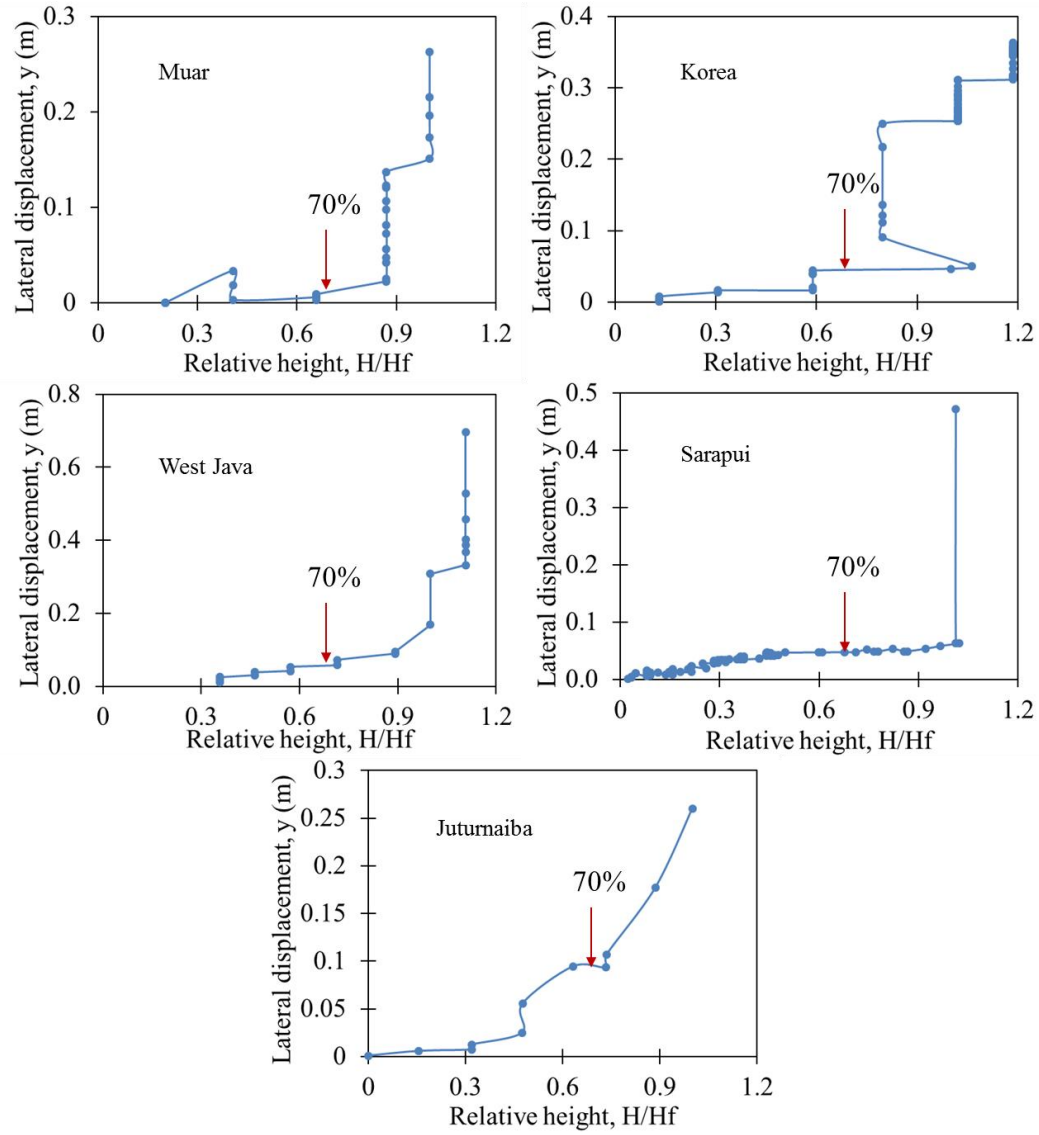

Figure 5.7 Failure analysis of all 5 datasets by Hunter and Fell

5.8 Coutinho and Bello [4]

Corresponding methodology proposes two failure criterion, first being the lateral displacement normalized by the depth of the clay layer, and the second is the rate of the lateral displacement normalized by the depth of the clay layer. Both can be

observed from the Figure 5.8. The first failure criterion is y/D > 1.2% (the y axis), the second is Δ(y/D)/Δt > 0.2% (the slope of the plot). Both criteria can be applied to all methodologies. However, the results according to the first criterion are more conservative (failure occurs earlier) in comparison to the second. Therefore, the results based on the second criterion were used for furhter evaluation. In the Figure 5.8, the slopes at the failure point and point before failure are shown.

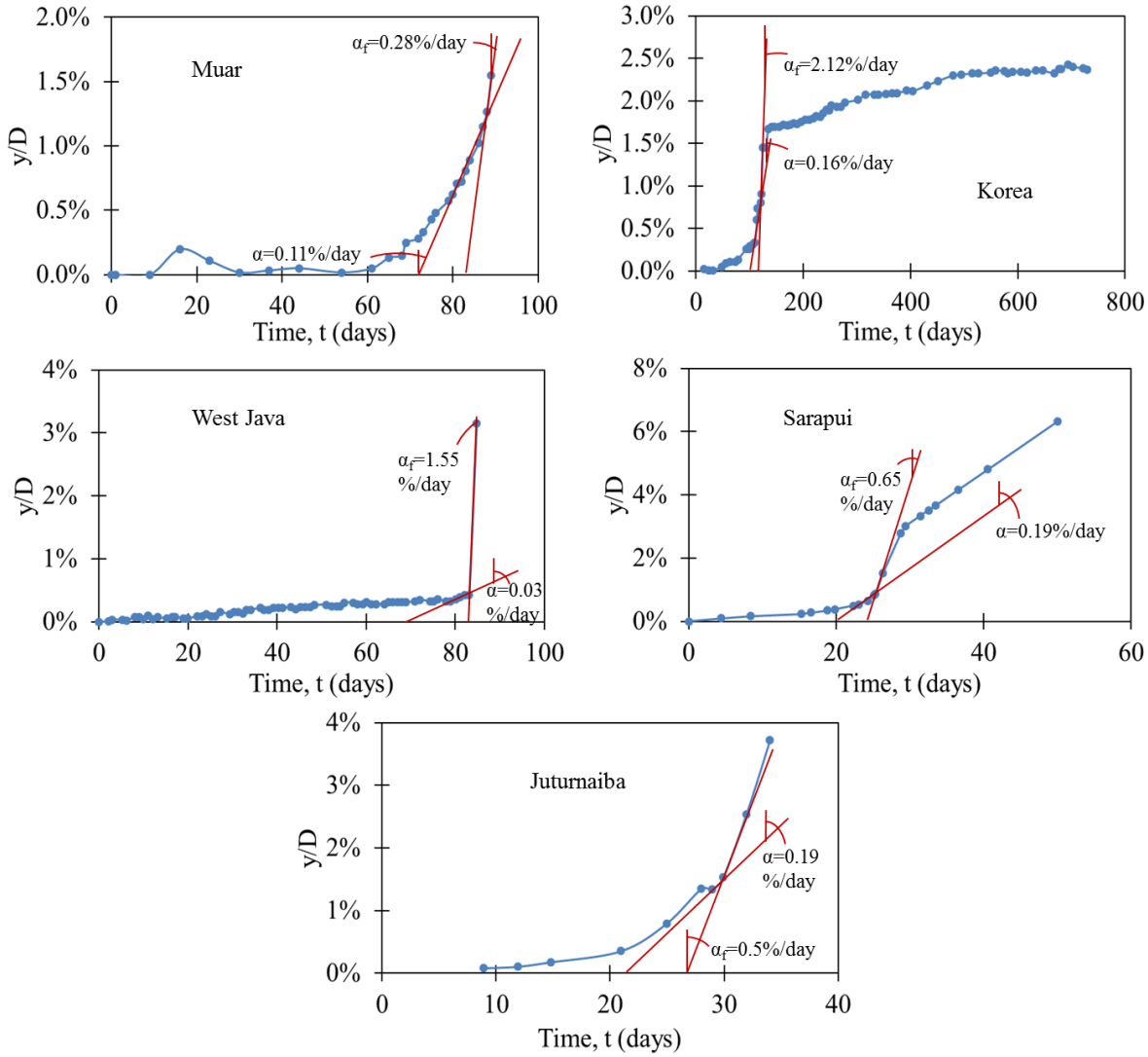

Figure 5.8 Failure analysis of all 5 datasets by Coutinho and Bello

5.9 Trani and Wong [5]

The failure analysis is conducted using the plot of the inverse incremental lateral displacement against the embankment height. The point where the inverse incremental lateral displacement is equal to or lower than 0.01 mm/day is the failure point. The Figure 5.9 illustrates the failure point and corresponding failure heights of the embankments. The red dotted line is trendline of the plot that makes it easier to detect the failure point.

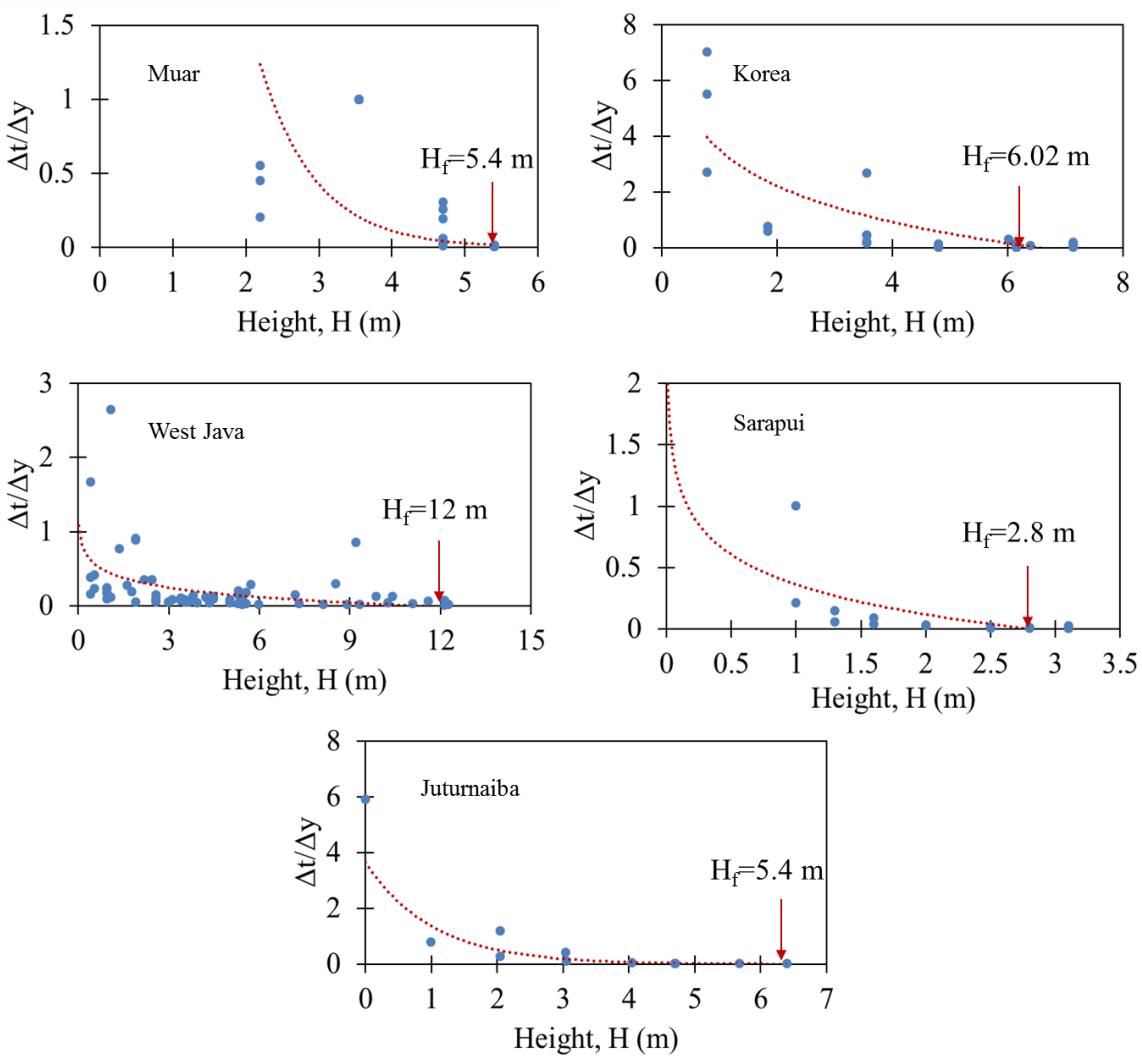

Figure 5.9 Failure analysis of all 5 datasets by Trani and Wong

5.10 Otoko [10]

According to Otoko, the failure heights of the embankments can be easily calculated using simplified equation (5),

$$H_f = \frac{3*C_u}{\gamma}, \quad (5)$$

where C_u is the undrained shear strength clay;

γ is the unit weight of the clay.

(i) Muar: C_u = 25 kPa; γ = 16 kN/m^3;

$$H_f = \frac{3*25}{16} = 4.7\ m.$$

(ii) Korea: C_u = 23 kPa; γ = 16 kN/m^3;

$$H_f = \frac{3*23}{16} = 4.4\ m$$ – not applicable.

(iii) West Java: C_u = 45 kPa; γ = 16 kN/m^3;

$$H_f = \frac{3*45}{16} = 8.5\ m.$$

(iv) Sarapui: C_u = 11 kPa; γ = 16 kN/m^3;

$$H_f = \frac{3*11}{16} = 2.0\ m.$$

(v) Juturnaiba: C_u = 25 kPa; γ = 16 kN/m^3;

$$H_f = \frac{3*25}{16} = 4.7\ m.$$

6 Discussions

6.1 Summary

Table 6.1 shows the summary of the analysis part. In this table the efficiencies based on the failure heights of the applied methodologies are presented. It is derived from the fact whether the resulted failure height matched the actual failure height or not. From such perspective, the stability prediction method by Matsuo and Kawamura [6] shows the best efficiency with 100 % matching. The worst efficiency of 0 % is resulted by Otoko [10].

Table 6.1 Summary of the prediction methods' application

#		Muar	Korea	West Java	Sarapui	Juturnaiba	efficiency
1	Matsuo and Kawamura [6]	1	1	1	1	1	100%
2	Kurihara and Ichimoto [17]	1	1	1	0	0	60%
3	Tominaga and Hashimoto [17]	1	0	1	1	0	60%
4	Calvacante, Coutinho and Gusmao [3]	0	0	1	0	1	40%
5	Coutinho and Bello [4]	1	0	1	1	0	60%
6	Ortigao, Werneck and Lacerda [8]	0	0	1	0	0	20%
7	Tavenas and Leroueil [18]	0	0	1	0	0	20%
8	Hunter and Fell [7]	0	1	0	0	0	20%
9	Trani and Wong [5]	1	1	1	0	1	80%

10	Otoko [10]	0	0	0	0	0	0%

6.2 Observations and recommendations

Table 6.2 shows the evaluation of the methodologies in terms of exact failure height efficiency. In other words, it shows how far or how close the resulted value from the actual field results. The evaluation is carried out only for methodologies that did not predict the failure height.

Kurihara and Ichimoto [17] methodology resulted in 60% efficiency, giving conservative results for the rest 40%. In terms of the magnitude of the failure height, it shows 94% efficiency, which is good. If the failure criterion for this method is increased from 20 mm/day to 40 mm/day, it could predict the exact failure heights for all case studies, except for Korea. 40 mm/day failure criterion do not detect the failure in Korean embankment.

The methodology proposed by Tominaga and Hashimoto [17] shows 60% efficiency in predicting failure and 94% efficiency in predicting the failure height, similarly to Kurihara and Ichimoto [17]. The issue is the fact that the given method has overestimated the strength of the Korean embankment. It is assumed that the accuracy will be higher with more readings from measurements.

It was observed that in Coutinho and Bello [4] method the second failure criterion based on the rate of the lateral displacement normalized by the depth of the soft soil gives more accurate results than the first criterion. The accuracy of the second

failure criterion could be the result of narrowing the failure range. In case of Calvacante, Coutinho and Gusmao [3] methodology, in the opposite, the first criterion based on the angular distortion gives better outputs than the second criterion based on the rate of the angular distortion. It is assumed that the second criterion would be more accurate if the time lag of the measurements is the same.

Ortigao, Werneck and Lacerda [8] method have predicted the failure only in one case, showing 20% efficiency. The case that was predicted is West Java fill with a sudden increase in lateral displacement, thus, it is assumed that the methodology should be revised. In terms of predicting the magnitude of the failure height, it showed 63% efficiency, overestimating the strength of the Korean embankment, as well.

The second failure criterion of Tavenas and Leroueil [18] based on the excess pore pressure was able to detect the failure properly only on West Java case, showing 20% efficiency. In predicting the failure height, it resulted in the lowest efficiency, as it could not detect the failure in 3 datasets. It is assumed that the reason could be the amount of the measurement readings, which could lead to low accuracy.

Hunter and Fell [7] predicted the failure only in West Java fill the case and showed very conservative values in other cases. It could be due to the failure criterion that is assumed to be too general and has low accuracy.

The second-best results are illustrated by Trani and Wong [5] method. It should be mentioned that the failure criterion was reduced to 0.01 mm/day since the literature review stated the approximate value of 0.05 mm/day. It is observed that the value of 0.015 mm/day would have resulted in 100% efficiency.

Among the reviewed methodologies, the proposals of Calvacante, Coutinho and Gusmao [3], Tavenas and Leroueil [18] and Otoko [10] were not able to detect the failure in some cases. In addition, Otoko [10] resulted in conservative values in all cases, thus having 0% efficiency. This method is also assumed to be too general with low accuracy.

Table 6.2 The efficiency of the methodologies to predict the exact failure height

#		Muar	Korea	West Java	Sarapui	Juturnaiba	efficiency
1	Matsuo and Kawamura [6]	-	-	-	-	-	-
2	Kurihara and Ichimoto [17]	-	-	12	2.5	6	94%
3	Tominaga and Hashimoto [17]	-	6.4	-	-	6	94%
4	Calvacante, Coutinho and Gusmao [3]	0	0	-	3.1	-	37%
5	Coutinho and Bello [4]	-	6.4	-	-	6	94%
6	Ortigao, Werneck and Lacerda [8]	4.7	6.4	-	1.6	0	63%
7	Tavenas and Leroueil [18]	0	0	-	3.1	0	28%
8	Hunter and Fell [7]	4.7	-	8.5	2	0	57%
9	Trani and Wong [5]	-	-	-	2.5	-	89%

10	Otoko [10]	4.7	0	8.5	2	0	46%

Table 6.3 shows the type of parameter used in reviewed techniques. It can be seen that the lateral displacement is applied the most among methodologies. In addition to the recommendations given above, it should be mentioned that the accuracy of the methodologies that applied the relative height of the embankment is low. In the contrary the methods using the lateral displacement have higher accuracy. Thus, it is assumed that the lateral displacement is the most suitable parameter to describe the stability of the embankments on soft clays.

Table 6.3 List of the parameters by methodologies

#		s	y	d	θ	H	σ'	Δu	z
1	Matsuo and Kawamura [6]	1	1						
2	Kurihara and Ichimoto [17]		1						
3	Tominaga and Hashimoto [17]	1	1						
4	Calvacante, Coutinho and Gusmao [3]			1	1				
5	Ortigao, Werneck and Lacerda [8]		1			1	`		
6	Tavenas and Leroueil [18]	1	1				1	1	
7	Hunter and Fell [7]		1		1	1			1
8	Coutinho and Bello [4]		1	1					
9	Trani and Wong [5]		1			1			
10	Otoko [10]						1		
Total		3	8	2	2	3	2	1	1

7 Conclusion

Summing up the work done, it was found that the numerical simulation can be applied to evaluate the stability of the embankments on soft clays. The Soft Soil Model is assumed to be the best soil constitutive model to describe the behaviour of the soft clays. In addition, the simulations revealed that the application of the Hardening Soil Model is not suitable to characterize the soft clay in terms of lateral displacement.

Among the 10 reviewed embankment stability prediction methodologies, the best technique is assumed to be Matsuo and Kawamura counter lines. The case studies that were carried out showed that this methodology predicted the embankment failure in all 5 cases. The worst stability evaluation method is proposed by Otoko, which is based on the simple equation. It is supposed that the simplicity of this equation lowers its accuracy, thus showing low efficiency.

The failure of the West Java fill case was predicted the most. It is due to the occurrence of the sudden failure that resulted in high differences in both settlement and lateral displacement. Therefore, it is easier to detect the failure.

Based on the case study analysis several recommendations were made for reviewed empirical methods to increase their accuracy:

(i) Increase the number of measurement readings to improve the accuracy of stability evaluation;

(ii) Use the same time lags for incremental measurements.

It was also found that the evaluation techniques based on the height have low accuracy, whereas the methodologies applying lateral displacement have high accuracy. In addition, the observations revealed that the majority of the embankment stability assessment methods use the lateral displacement at the embankment toe. Thus, it can be concluded that the lateral displacement describes the soft clay behaviour the best. It can be used for further investigations to increase the accuracy of the existing empirical methods or to develop a new methodology.

8 References

[1]Research Designs and Standards Organisation, "GUIDELINES ON SOFT SOILS-STAGE CONSTRUCTION METHOD", GOVERNMENT OF INDIA MINISTRY OF RAILWAYS, 2005.

[2]Z. Habibnezhad, "Stability Analysis of Embankments Founded on Clay - a comparison between LEM & 2D/3D FEM", MSc Thesis, Royal Institute of Technology, 2014.

[3]S. Cavalcante, R. Coutinho and A. Gusmão, "Analysis of Behavior of Embankments on Soft Soils Geotechnical Investigations and Instrumentation Access of Embank Ments the Jitituba River Bridge", in *Fifth International Conference on Case Histories in Geotechnical Engineering*, New York, 2004.

[4]R. Coutinho and M. Bello, "Analysis and Control of the Stability of Embankments on Soft Soils: Juturnaíba and others Experiences in Brazil", *Soils and Rocks*, vol. 4, no. 31, pp. 331-351, 2011.

[5]D. Trani and P. Wong, "PREDICTING INSTABILITY OF EMBANKMENTS ON SOFT GROUND FROM MONITORING DATA", *Australian Geomechanics*, vol. 49, no. 3, 2014.

[6]Matsuo, M., and Kawamura, K., 1977, “Diagram for construction of embankment on soft ground,” Soils and Foundations, 17 (3), pp. 37-52.

[7] Hunter, G., and Fell, R., 2003, "Prediction of impending failure of embankments on soft ground," Canadian Geotechnical Journal, 40(1), pp. 209-220.

[8] Ramalho-Ortigão, J. A., Werneck Mauro, L. G., and Lacerda Willy, A., 1983, "Embankment Failure on Clay near Rio de Janeiro," Journal of Geotechnical Engineering, 109(11), pp. 1460-1479.

[9]Plaxis, "Material Models Manual", 2016. [Online]. Available: https://www.plaxis.com/product/plaxis-2d/. [Accessed: 28- Oct- 2017].

[10]G. Otoko, "Analysis of the stability of embankments on clay foundations", International Journal of Engineering and Technology Research, vol. 2, no. 1, pp. 1-11, 2014.

[11] Ladd Charles, C., 1991, "Stability Evaluation during Staged Construction," Journal of Geotechnical Engineering, 117(4), pp. 540-615.

[12] de Souza S. Almeida, M., and Marques, M. E. S., 2013, Design and Performance of Embankments on Very Soft Soils, Taylor & Francis.

[13]S. Leroueil, "Embankments on Soft Clays", in CIGMAT, Houston, Texas, 2006.

[14]J. Chu, D. Bergado, E. Shin and J. Chai, "EMBANKMENTS ON SOFT GROUND AND GROUND IMPROVEMENT", in GEOSYNTHETICS ASIA, Bangkok, Thailand, 2012.

[15] Peck, R. B., 1969, "Advantages and Limitations of the Observational Method in Applied Soil Mechanics," Géotechnique, 19(2), pp. 171-187.

[16]R. Fell, O. Hungr, S. Leroueil and W. Riemer, "KEYNOTE LECTURE – GEOTECHNICAL ENGINEERING OF THE STABILITY OF NATURAL SLOPES, AND CUTS AND FILLS IN SOIL", in International conference on geotechnical and geological engineering, Melbourne, Australia, 2000.

[17]H. Todo, T. Sagae, M. Yamaguchi and Y. Chandra, "Comparison of Stability Control Methods for Embankments on Soft Ground in Southeast Asia", in Twelfth Southeast Asian Geotechnical Conference, Kuala Lumpur, Malaysia, 1996.

[18] Tavenas, F., and Leroueil, S., 1980, "The behaviour of embankments on clay foundations," Canadian Geotechnical Journal, 17(2), pp. 236-260.

[19]A. Bin Abd Aziz, "Stability and Deformation Analysis of Embankment on Soft Clay", Undergraduate, Universiti Teknologi Malaysia, 2010.

[20]B. Huat, "Behaviour of Soft Clay Foundation beneath an Embankment", Pertanika Journal of Science & Technology, vol. 2, no. 2, pp. 215-235, 1994.

[21]"PLAXIS 2D - Plaxis", Plaxis, 2017. [Online]. Available: https://www.plaxis.com/product/plaxis-2d/. [Accessed: 25- Nov- 2017].

[22] Almeida, M.S.S. and Marques, M.E.S., 2003. The behaviour of Sarapuí soft clay. Characterization and engineering properties of natural soils. Edited by TS Tan, KK Phoon, DW Hight, and S. Leroueil. Swets & Zeitlinger, Lisse, the Netherlands, pp.477-504

[23] Indraratna, B., Balasubramaniam, A.S. and Balachandran, S., 1992. Performance of test embankment constructed to failure on soft marine clay. Journal of Geotechnical Engineering, 118(1), pp.12-33.

[24] Kim, J.S., Chang, Y.C. and Park, S.S., 2013. A development of embankment stability evaluation method on soft foundation. Journal of the Korean Geotechnical Society, 29(9), pp.43-54.

[25] Das, B. (2007). Principles of Foundation Engineering. Boston: PWS Engineering.

Appendices

8.1.1 Appendix A

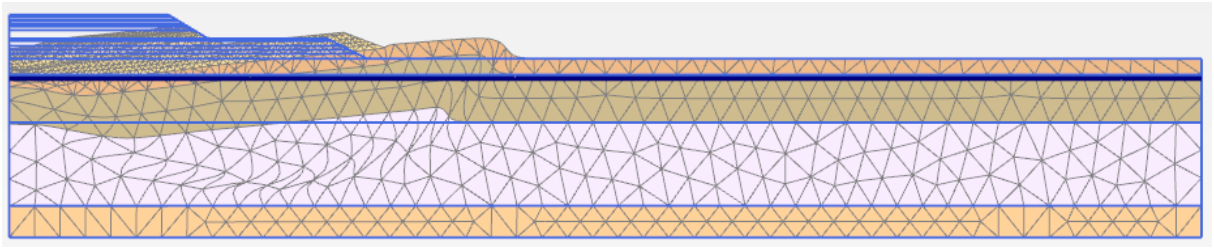

Figure A.1 Deformed mesh of the test embankment (SS model)

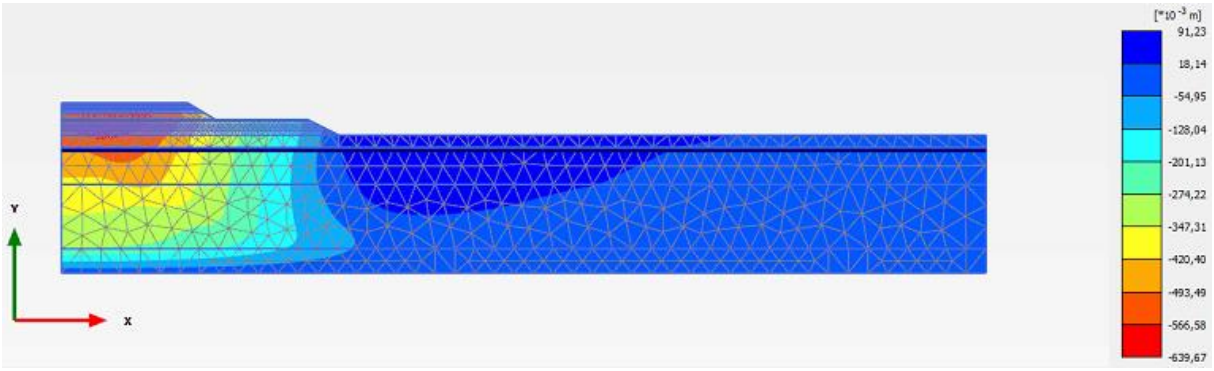

Figure A.2 Vertical deformation map of the test embankment (SS model)

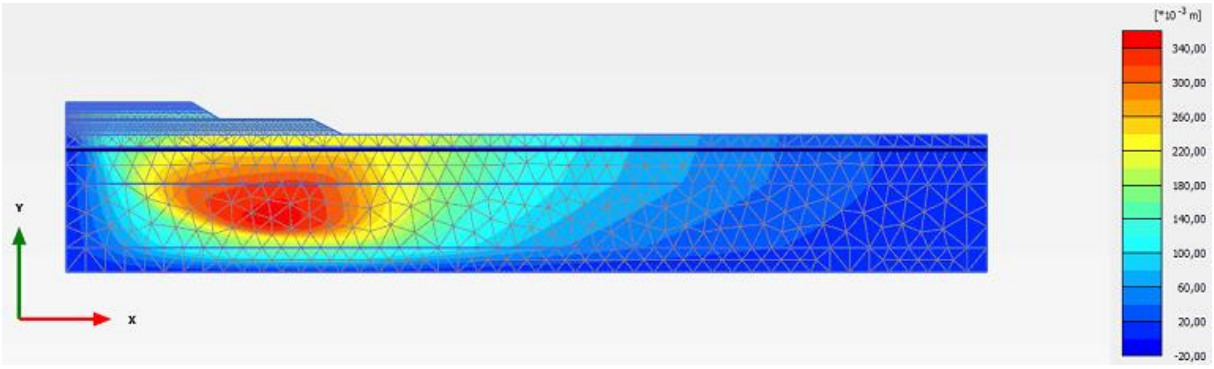

Figure A.3 Horizontal deformation map of the test embankment (SS model)

Table A.1 Settlement at the center of the test embankment (SS model)

Point	Step	Time [day]	u_y [m]
0	0	0.0	0.000
1	15	0.0	0.000
2	15	2.0	-0.010
3	16	4.0	-0.023
4	1	6.0	-0.027
5	2	8.0	-0.030
6	3	10.0	-0.040
7	4	12.0	-0.051
8	17	19.0	-0.061
9	18	26.0	-0.065
10	5	29.0	-0.075
11	6	32.0	-0.088
12	7	34.0	-0.092
13	8	36.0	-0.096
14	9	37.5	-0.107
15	10	39.0	-0.121
16	19	42.5	-0.134
17	20	46.0	-0.143
18	281	49.5	-0.198
19	282	53.0	-0.264
20	283	59.6	-0.290
21	284	69.0	-0.309
22	25	70.0	-0.328
23	26	71.0	-0.348
24	11	73.0	-0.356
25	12	75.0	-0.362
26	27	77.0	-0.382
27	28	79.0	-0.404
28	13	80.5	-0.409
29	14	82.0	-0.413
30	285	82.5	-0.429
31	286	83.0	-0.447
32	21	83.5	-0.450
33	22	84.0	-0.452
34	287	84.5	-0.463
35	288	84.8	-0.469
36	289	84.8	-0.470
37	290	84.8	-0.470
38	291	84.9	-0.471
39	292	84.9	-0.472
40	293	85.0	-0.472
41	23	85.5	-0.475
42	24	86.0	-0.477
43	294	86.5	-0.498
44	295	86.6	-0.505
45	296	86.6	-0.507
46	297	86.6	-0.509
47	298	86.7	-0.511
48	299	86.7	-0.513
49	300	86.7	-0.514
50	301	86.8	-0.516
51	302	86.8	-0.517
52	303	86.8	-0.519
53	304	86.9	-0.522
54	305	86.9	-0.526
55	306	87.0	-0.530
56	29	87.5	-0.533
57	30	88.0	-0.537
58	307	88.3	-0.544
59	308	88.3	-0.548
60	309	88.3	-0.551
61	310	88.3	-0.556
62	311	88.3	-0.558
63	312	88.3	-0.560
64	313	88.3	-0.562
65	314	88.4	-0.563
66	315	88.4	-0.564
67	316	88.4	-0.565
68	317	88.4	-0.566
69	318	88.5	-0.568
70	319	88.5	-0.570
71	320	88.5	-0.573
72	321	88.5	-0.574
73	322	88.5	-0.577
74	323	88.6	-0.579
75	324	88.6	-0.582
76	325	88.6	-0.584
77	326	88.6	-0.589
78	327	88.6	-0.591
79	328	88.6	-0.597
80	329	88.6	-0.601

Table A.2 Lateral displacement at the test embankment toe (SS model)

Point	Step	Time [day]	u_x [m]
0	0	0.0	0.000
1	15	0.0	0.000
2	15	2.0	0.005
3	16	4.0	0.010
4	1	6.0	0.008
5	2	8.0	0.007
6	3	10.0	0.011
7	4	12.0	0.016
8	17	19.0	0.013
9	18	26.0	0.011
10	5	29.0	0.017
11	6	32.0	0.023
12	7	34.0	0.022
13	8	36.0	0.022
14	9	37.5	0.031
15	10	39.0	0.042
16	19	42.5	0.039
17	20	46.0	0.038
18	281	49.5	0.056
19	282	53.0	0.079
20	283	59.6	0.075
21	284	69.0	0.074
22	25	70.0	0.082
23	26	71.0	0.091
24	11	73.0	0.091
25	12	75.0	0.091
26	27	77.0	0.098
27	28	79.0	0.107
28	13	80.5	0.107
29	14	82.0	0.107
30	285	82.5	0.116
31	286	83.0	0.130
32	21	83.5	0.130
33	22	84.0	0.130
34	287	84.5	0.136
35	288	84.8	0.143
36	289	84.8	0.145
37	290	84.8	0.149
38	291	84.9	0.150
39	292	84.9	0.152
40	293	85.0	0.154
41	23	85.5	0.154
42	24	86.0	0.154
43	294	86.5	0.165
44	295	86.6	0.172
45	296	86.6	0.176
46	297	86.6	0.180
47	298	86.7	0.183
48	299	86.7	0.185
49	300	86.7	0.188
50	301	86.8	0.190
51	302	86.8	0.192
52	303	86.8	0.194
53	304	86.9	0.198
54	305	86.9	0.202
55	306	87.0	0.206
56	29	87.5	0.206
57	30	88.0	0.206
58	307	88.3	0.209
59	308	88.3	0.213
60	309	88.3	0.216
61	310	88.3	0.221
62	311	88.3	0.223
63	312	88.3	0.226
64	313	88.3	0.228
65	314	88.4	0.230
66	315	88.4	0.231
67	316	88.4	0.233
68	317	88.4	0.236
69	318	88.5	0.239
70	319	88.5	0.242
71	320	88.5	0.246
72	321	88.5	0.249
73	322	88.5	0.252
74	323	88.6	0.256
75	324	88.6	0.260
76	325	88.6	0.263
77	326	88.6	0.269
78	327	88.6	0.273
79	328	88.6	0.281
80	329	88.6	0.285

8.1.2 Appendix B

Table B.2 Analysis results for Muar test embankment

	s (mm)			y (mm)			Hf (mm)
Field	616.3	|Δ|	(%)	262.9	|Δ|	(%)	5400
T&H	596.5	19.8	3.2%	215.4	47.5	18.1%	5400
K&I	588.2	28.2	4.6%	195.8	67.1	25.5%	5400
M&K	616.3	0.0	0.0%	262.9	0.0	0.0%	5400
O,W&L	529.0	87.3	14.2%	137.1	125.8	47.9%	4700
T&L	N/A	N/A	N/A	N/A	N/A	N/A	N/A
H&F	335.1	281.2	45.6%	22.4	240.6	91.5%	4700
C,C&G	N/A	N/A	N/A	N/A	N/A	N/A	N/A
C&B	616.3	0.0	0.0%	262.9	0.0	0.0%	5400
T&W	596.5	19.8	3.2%	215.4	47.5	18.1%	5400
O/C	335.1	281.2	45.6%	22.4	240.6	91.5%	4700

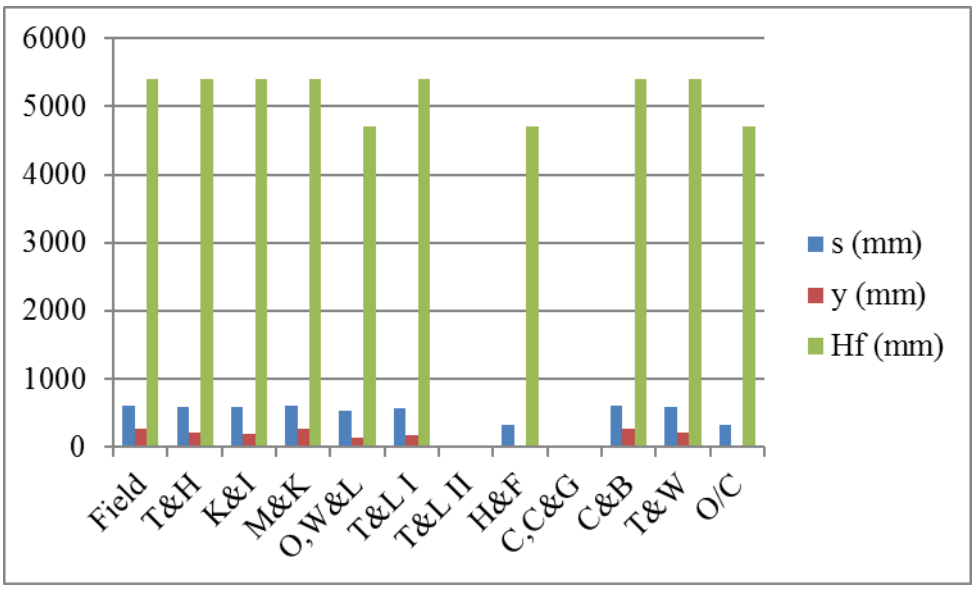

Figure B.2 Embankment parameters for Muar test embankment

Table B.3 Analysis results for Korean embankment

	s (mm)			y (mm)			Hf (mm)
Field	258.8	|Δ|	(%)	136.3	|Δ|	(%)	6020
T&H	288.8	30.0	11.6%	217.0	80.7	59.2%	6400
K&I	258.8	0.0	0.0%	136.3	0.0	0.0%	6020
M&K	258.8	0.0	0.0%	136.3	0.0	0.0%	6020

O,W&L	288.8	30.0	11.6%	217.0	80.7	59.2%	6400
T&L	N/A	N/A	N/A	N/A	N/A	N/A	N/A
H&F	258.8	0.0	0.0%	136.3	0.0	0.0%	6020
C,C&G	N/A	N/A	N/A	N/A	N/A	N/A	N/A
C&B	288.8	30.0	11.6%	217.0	80.7	59.2%	6400
T&W	258.8	0.0	0.0%	136.3	0.0	0.0%	6020
O/C	N/A	N/A	N/A	N/A	N/A	N/A	N/A

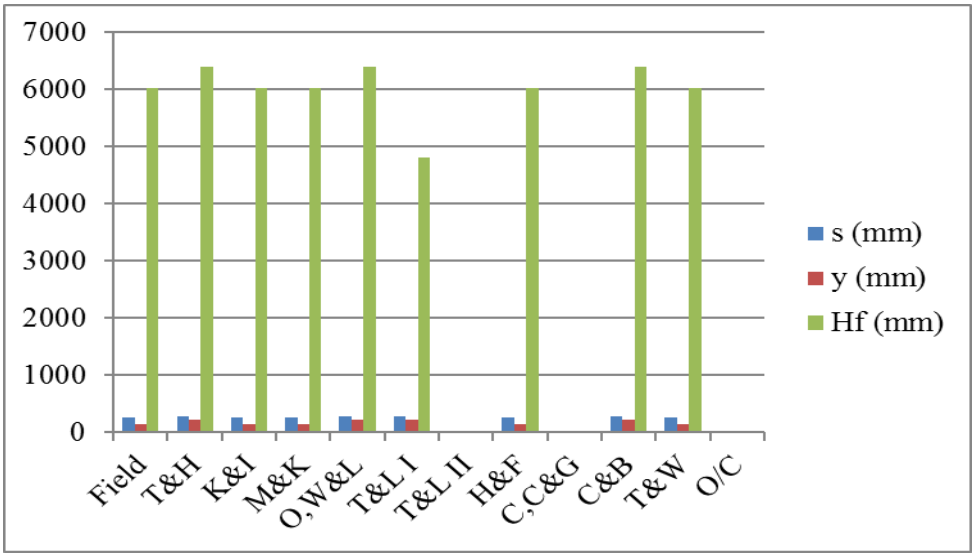

Figure B.3 Embankment parameters for Korean embankment

Table B.4 Analysis results for West Java fill

	s (mm)			y (mm)			Hf (mm)
Field	1188.3	|Δ|	(%)	472.5	|Δ|	(%)	12000
T&H	909.7	278.6	23.4%	63.1	409.4	86.6%	12000
K&I	1188.3	0.0	0.0%	472.5	0.0	0.0%	12000
M&K	1188.3	0.0	0.0%	472.5	0.0	0.0%	12000
O,W&L	1188.3	0.0	0.0%	472.5	0.0	0.0%	12000
T&L	1188.3	0.0	0.0%	472.5	0.0	0.0%	12000
H&F	650.9	537.4	45.2%	41.8	430.7	91.2%	8500
C,C&G	1188.3	0.0	0.0%	472.5	0.0	0.0%	12000
C&B	1188.3	0.0	0.0%	472.5	0.0	0.0%	12000
T&W	1188.3	0.0	0.0%	472.5	0.0	0.0%	12000
O/C	650.9	537.4	45.2%	41.8	430.7	91.2%	8500

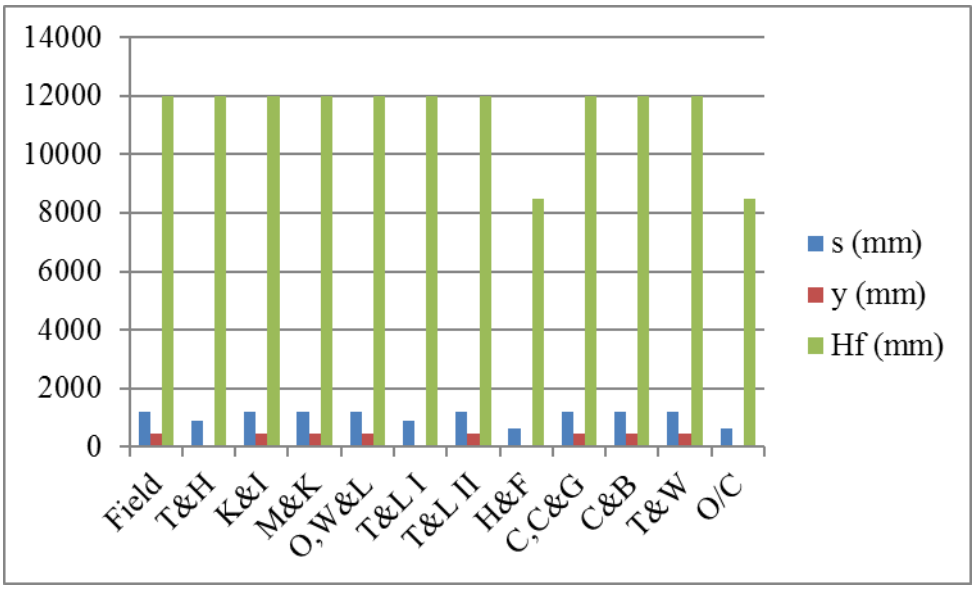

Figure B. 4 Embankment parameters for West Java fill

Table B. 5 Analysis results for Sarapui test embankment

	s (mm)			y (mm)			Hf (mm)
Field	416.3	|Δ|	(%)	307.5	|Δ|	(%)	2800
T&H	283.4	132.9	31.9%	168.7	138.8	45.1%	2800
K&I	210.6	205.7	49.4%	89.7	217.8	70.8%	2500
M&K	416.3	0.0	0.0%	307.5	0.0	0.0%	2800
O,W&L	125.1	291.2	69.9%	53.5	254.0	82.6%	1600
T&L	1086.3	670.0	160.9%	366.7	59.2	19.3%	3100
H&F	142.2	274.1	65.8%	57.6	249.9	81.3%	2000
C,C&G	484.9	68.6	16.5%	331.6	24.1	7.8%	3100.0
C&B	283.4	132.9	31.9%	168.7	138.8	45.1%	2800
T&W	232.0	184.3	44.3%	95.2	212.3	69.0%	2500
H&F	142.2	274.1	65.8%	57.6	249.9	81.3%	2000

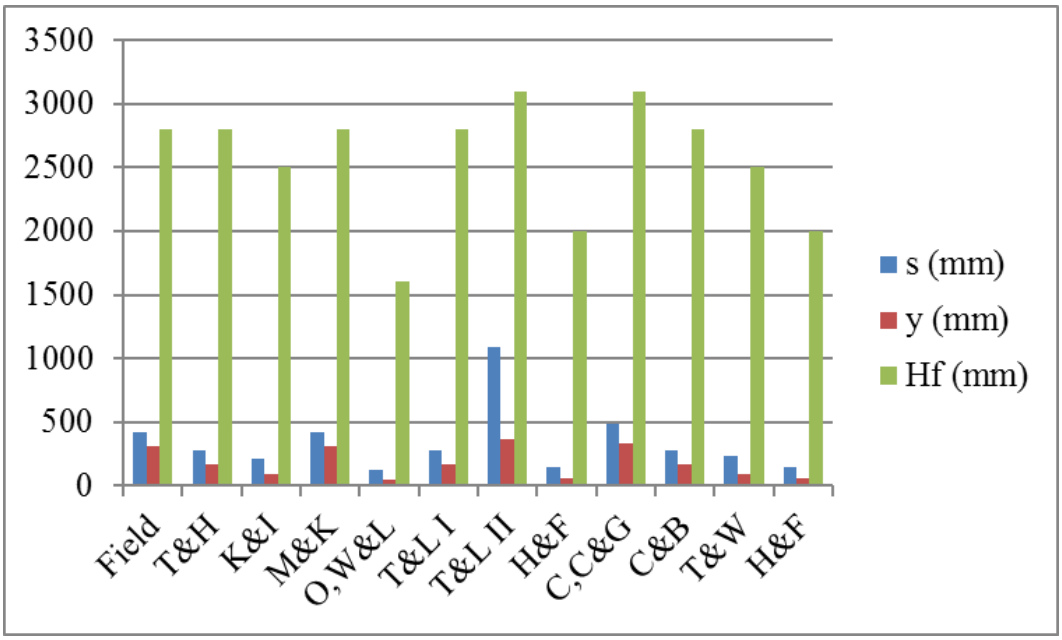

Figure B.5 Embankment parameters for West Java fill

Table B.6 Analysis results for Juturnaiba test embankment

	s (mm)			y (mm)			Hf (mm)
Field	502.3	|Δ|	(%)	198.6	|Δ|	(%)	6400
T&H	469.3	33.0	6.6%	159.5	39.1	19.7%	6000
K&I	469.3	33.0	6.6%	159.5	39.1	19.7%	6000
M&K	502.3	0.0	0.0%	198.6	0.0	0.0%	6400
O,W&L	469.3	33.0	6.6%	159.5	39.1	19.7%	6000
T&L	469.3	33.0	6.6%	159.5	39.1	19.7%	6000
H&F	374.7	127.6	25.4%	85.5	113.1	57.0%	4700
C,C&G	502.3	0.0	0.0%	198.6	0.0	0.0%	6000
C&B	469.3	33.0	6.6%	159.5	39.1	19.7%	6000
T&W	502.3	0.0	0.0%	198.6	0.0	0.0%	6400
O/C	374.7	127.6	25.4%	85.5	113.1	57.0%	4700

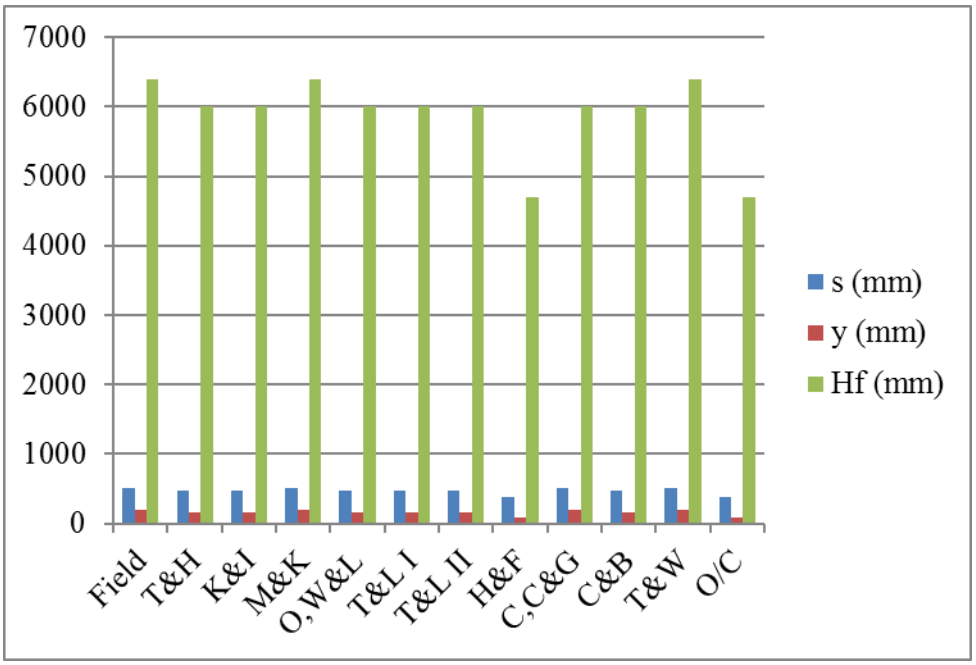

Figure B.6 Embankment parameters for Juturnaiba test embankment